EFFECT OF SPACE RADIATION ON COMPOSITE MATERIAL THAT WAS INTERNAL AND EXTERNAL OF THE PRESSURIZED VOLUME ON THE INTERNATIONAL SPACE STATION (ISS)

07/2022

By

IAN D JUBY

Bachelor of Science in Mechanical Engineering

Oklahoma State University

Tulsa, OK

2013

Submitted to the Faculty of the Graduate College of the Oklahoma State University in partial fulfillment of the requirements for the Degree of MASTER OF SCIENCE
JULY, 2022

EFFECT OF SPACE RADIATION ON COMPOSITE MATERIAL THAT WAS INTERNAL AND EXTERNAL OF THE PRESSURIZED VOLUME ON THE INTERNATIONAL SPACE STATION (ISS)

Thesis Approved:

Thesis Adviser

Dr. Ranji Vaidyanathan

Dr Raman Singh

Dr. Eric Benton

ACKNOWLEDGEMENTS

A lot of sacrifices were made by many people in my life on my path to completing my degree and this research and would like to acknowledge them in this section. To God for me giving the will and patience to continue down the path of my education and completing this research. To my wife Jessica, you have supported me throughout this journey and chapter in our lives by allowing me to work on this degree and research for many seasons of our lives together. Our family has increased with the birth of our beautiful children and the responsibilities inside our home increased tremendously and you have continued to support me and urged me to finish. To my children, Creedon, Paxton and Iana, you have all made sacrifices of time for me, allowing me to work long hours after work and on weekends. I would like to thank my parents David and Brenda Juby for continue to press me to advance my learning to the next level and their support through it all. Even though you're no longer alive Dad, completing this is an accomplishment that I know you would be proud of. Also a thanks to Tia Juby for pushing me forward in a sibling competitive spirit. I would like to thank Bill and Melissa Fishburn for all the support and accountability in pushing me to finish what I started. I would like to thank my colleagues at NASA, Nathanael Greene and Aaron Laney for continuing to press me forward and the encouragement you gave me through the frustrating times and for helping to take workloads off me, to dedicate time to this research. I would also like to express my deepest gratitude to Dr. Ranji Vaidyanathan for keeping me accountable with my goals of finishing my masters and always encouraging me through all of the hort comings that I have faced along the way. You made this possible with providing your labs and staff to help run experiments, when all my other resources had evaporated due to the pandemic. You told me not to worry and presented me with options and solutions. I would like to thank Dr. Eric Benton for his expertise and willingness to give the only coupons that he had from the MISSE-11 experiments and run testing on, in order to provide insight into the effect of space radiation on composites in external environments. Also for supplying the time of your staff to run prediction models of radiation doses. I am very grateful for everything you did for me in my time of need. I want to thank Dr. Raman Singh for taking time to serve on my committee and review of my research. Lastly, I want to thank Martin Yang for performing the OLTARIS models for the MISSE coupons and Siddhesh Chaudhari for performing the experimental work on all the coupons sets. Everyone mentioned above served a crucial part in this process and I will never forget all that you have done. As my father said, "never forget where you came from, or you will forget who you have become and who helped you get there"

Name: IAN DAVID JUBY

Date of Degree: JULY 2022

Title of Study: EFFECT OF SPACE RADIATION ON COMPOSITE MATERIAL THAT WAS INTERNAL AND EXTERNAL OF THE PRESSURIZED VOLUME ON THE INTERNATIONAL SPACE STATION (ISS)

Major Field: MATERIALS SCIENCE AND ENGINEERING

Abstract

The focus of this study will be on the effects that radiation environments on ISS have on composite coupons. Coupons from two different experimental programs HiMassSEE and MISSE-11 were used to run testing on. The HiMassSEE coupons were internal to the pressurized volume and had high atomic number metallic foils in between the coupons to enhance the possibility of high energy secondary particle impacts. These impacts were seen on CR-39/Mica coupons that were processed by the material labs at Johnson Space Center. The concern with secondary impacts is how it effects the performance of the composite and whether there is a concern of early failure. The MISSE-11 coupons were primarily used for structural support for SC2020 coupons which were HDPE coupons with BN blended into the coupons. However there was interest in how being external to ISS would affect the mechanical properties of the carbon fiber coupons without shielding. Various tests were performed on each coupon set, unfortunately due to limitation of dimensions and quantity of coupons, side by side comparison of results of the HiMassSEE and MISSE-11 coupons could not be performed. For the HiMassSEE coupons, Differential Scanning Calorimetry (DSC), Fourier transform infrared Spectroscopy (FTIR) and Scanning Electron Microscopy (SEM) were performed. The DSC results demonstrated that the coupons were fully cross-linked prior to being flown and showed no enhanced cross-linking on top of what the ground controls showed. The FTIR results showed that there were increases in the aromatic ring structures and oxidation which suggests that enhanced chain scission was occurring on the surface of the coupons. There was also a distinct increase in absorbance peaks on each of the coupons in order of the atomic number (Z) which demonstrated that more activity within in the molecular structure of the coupons was occurring. The only coupon to not have these increases, but instead decreased in absorbance were the coupons with Niobium foils. Further studies are needed to determine that understanding of why this occurred. The SEM images for both the HiMassSEE and MISSE-11 coupons produced no signs of high energy particle impact in the form of track marks or epoxy degradation in which fibers were no longer adhered in the matrix. Dynamic mechanical analysis (DMA) showed the MISSE-11 coupons underwent very small changes in the material properties which could be contributed to cross-linking. The flight coupons demonstrated difference when compared to the ground controls, which was contributed to the orientated direction of the coupons. Both sets of experimental results displayed that radiation exposure in LEO provides negligible effects to composite performance. There does however still need to be research into the effect of radiation outside of LEO in deep space and lunar environments where the next generation of space exploration will occur.

TABLE OF CONTENTS

LIST OF FIGURES

LIST OF TABLES

CHAPTER I

INTRODUCTION

1.1 Motivation

Since the beginning of the space race in 1955 between the then Soviet Union and the United States of America, humans have had the desire and drive to explore the limits outside of earth's protective atmosphere. With what started as a competition during the Cold War, has continued with the idea of sustaining life in space and exploration. When Neil Armstrong and Buzz Aldrin landed on the moon in July of 1969 the world watched in wonder to what would be next. As the transmissions of Neil Armstrong's historical ladder descent to the lunar surface occurred and the one phrase that best described the event was "…one small step for a man, one giant leap for mankind" [1] After the Apollo 11 mission was completed the National Aeronautics and Space Administration (NASA), never turned back from the calling of space.

The International Space Station (ISS) has been in Low Earth Orbit (LEO) for over twenty-three years. ISS has been the central hub for research, development and sustained human life outside of earth atmosphere. After the developments of ISS were completed the next desire for NASA was to go further than before, by starting the Constellation program in 2003. Constellation was cancelled in 2010, however the framework of the program was already in place and was later restructured into a new program called Orion. In 2014

Exploration Flight Test-1 (EFT-1) launched out of Kennedy Space Center (KSC) and provided the path forward to get back to the moon by 2024 and to explore deeper into space than ever before.

With the drive to explore greater than ever before and mission profiles became more difficult, it was important to look at the materials being used for the structures, habitats, and subsystems of the spacecrafts. Composites have become the desired materials for space applications due to the weight constraints placed on designs in order to get the vehicles outside of earth atmosphere. Composites allow the designers to reduce weight without sacrificing structural integrity. Composites however are not without flaws and can be structurally compromised once outside of the earth's atmosphere where the environments are harsh and extreme. It is important that the environmental impacts surrounding these structures do not jeopardize or add risk to the crew or mission. NASA and the companies performing space flights invest large sums of money into studying different shielding materials and the protection they provide to the structures, crews, and payloads.

Throughout the mission, the space craft and crew will experience "three major forms of radiation exposure: galactic cosmic rays (GCR), solar particle events (SPE), and trapped radiation particles. GCR are particles that come from outside the solar system, but from within the Milky Way galaxy." [2] "GCR is composed of the nuclei of atoms that have had their surrounding electrons stripped away and are traveling at nearly the speed of light [2]. SPE are particles that are "produced by the acceleration across the transition shock

boundary of propagating coronal mass ejecta" [2]. "Trapped radiation occurs due to the Earth's magnetosphere. The "trapped" particles consist of protons, electrons, and heavier ions, and are known as the Van Allen belts [2]."

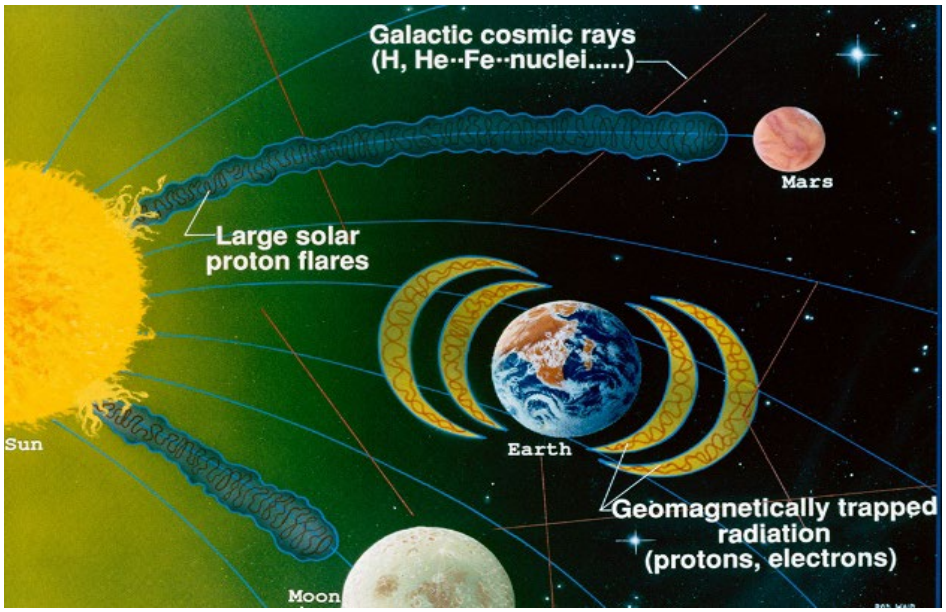

Figure 1: Space Radiation Exposure

On a spacecraft, GCRs are the most critical sources of radiation to the crew and avionic single events. It is a long-term constant environment. The spectra are harder to manage which makes shielding mass very impractical. [3,4] SPEs are transient events, which do not last for long periods of time. SPE can temporarily increase particle flux, Single Even Error or SEE rates and Traveling Ionospheric Disturbances or TID rates by orders of magnitude. [3,4] Because the energy spectra are considered to be "soft", managing the shielding mass on the spacecraft is much more practical than that of GCRs. "Trapped radiation is localized in space, consists primarily of energetic electrons (electron

belt) and protons (proton belt), and can drive annual dose rates as high a 10^5 cGy through 4 mm Al near geosynchronous equatorial orbit (GEO). Shielding is effective, even at 1 to 2 cm Al, but costly (up-mass). The very high flux of lower energy particles can determine surface dose of exposed materials." [3, 4].

1.2 Previous Studies

Different materials and how they are affected by radiation have been widely studied in multiple industries for ground source applications. The types of radiation however always have been limited sources, such as gamma radiation from radioisotopes (Cobalt-60 and Cesium-137) and electron beam radiation, both typically low in comparison to GCRs, SPEs and trapped radiation are found in deep space but can be much higher than seen in LEO [5]. The materials studied typically have not been manufactured for the purpose with use in aerospace applications. For applications in space, materials such as carbon fiber composites have traditionally focused on low earth orbit (LEO) and electron radiation at low energies [6, 7]. More recent studies have focused outside of the LEO and studied the effects of deep space radiation and lunar environments on structural composites [6, 7]. The following discussions outline some of the previous work that has been completed on irradiated polymers and composite structures and their effects of radiation on these materials. In most studies, the focus has been on the primary radiation effects on the materials versus the potential effects caused by secondary particle showers.

In general, it is a known fact that the direct effect of radiation on any given matter is to "ionize or excite the molecules of the irradiated matter" [8]. As molecules on the given matter become ionized and more excited, secondary effects can occur due to the ejection of electrons. When proton radiation is applied to a material, heavy ions collide with the atoms in the material creating incident ions. These ions create tracks in the materials which tend to grow radially outward due to the mechanism of secondary electrons produced due the ionization and excitation of the molecules [6,7]. This secondary electron production can then cause "spurs," which are areas of dense ionization. Because these areas that are already ionized and excited are very dense, the reaction of more paths off the original particle path can occur. These paths are called delta ray tracks. [6, 9]. Figure 2 illustrates the ion collision and its chain reactions effects. "The ionization in these tracks are locations of chemical changes that occur in the material as a result of energy transfers from the initial particle collisions and the electrons in which they interacted with" [6,7]. The chemical changes due to radiation that occur in polymer materials can consist of cross linking, chain scission and oxidation. [5, 6]. The chemical reaction in these materials can result in the degradation of physical properties. As electronic interactions occur in the material, protons begin to lose energy and the creation of free radicals occurs at the end of the molecules. The forming process of free radicals at the end of molecules creates the beginning stages of cross linking in the material [10]. Cross-linking in the material creates a mechanism in which the intermolecular bonds are linked together; the process initially stiffens the material and strengths it. But as the effect of cross-linking continues to increase the material

ultimately becomes brittle and unstable for load sharing. Chain Scission is the degradation of the main polymer chain and its side chains. Degradation due to oxidation occurs when oxygen is present, resulting in the formation of aldehydes, ketones, and carboxylic groups [5, 6, 8]. Figure 3 illustrates changes in a polymeric material due to proton irradiation [10].

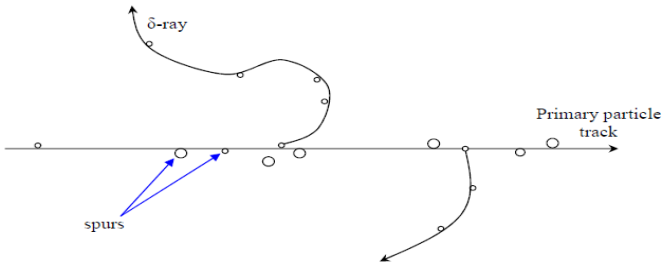

Figure 2: Ion collision and its chain reactions effects

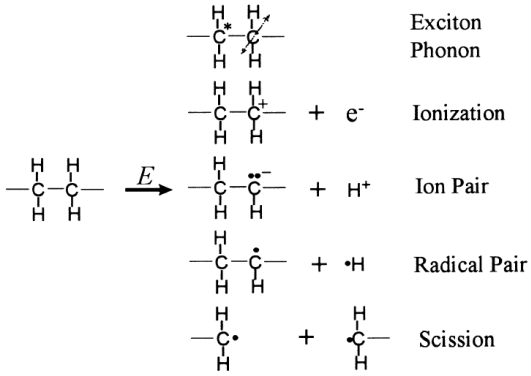

Figure 3: Changes in a polymeric material due to exposure to radiation

There are other studies which demonstrate that increasing amounts of aromatic polymers provide more radiation resistance. The reason for this is that their "ring structure absorbs excitation energy without concentrating it at a particular location within the molecule" [5, 6, 7, 11, 12, 13, 14]. However, this feature of these epoxies is less obvious when the samples are exposed to oxygen versus in vacuum. Multiple studies completed on

epoxies exposed to oxygen using Fourier Transform Infrared Spectroscopy (FTIR) have shown a significant increase in oxygen content on the composite surface. However, it was observed that this oxidation on the surface of the coupons affected the overall performance of the coupons very little. [6,7, 8].

Another study examined the effects of gamma radiation in an oxygen environment. The epoxy was a bisphenol A and the fiber was carbon. The dose rates were higher than that of LEO of 0.5,1 and 2 MGys. The results demonstrated a loss in modulus and fracture stress as well as a discoloration of the epoxy surface. The study showed that there was an increase in glass transition. Comparative studies of the different doses showed that higher the dose resulted in higher degradation. FTIR likewise showed an increase in absorbance peaks in multiple regions, including the carbonyl region which suggested that oxidation was occurring in the coupons. [6, 7, 15]

1.3 Motivation for the Present Study

The reason for the present study was that prior research has shown that composites degrade with high doses of focused radiation resulting from high energy particle accelerators. The problem with these studies is that while they provided fundamental knowledge into the extremes of composite degradation, they did not fully represent composite degradation that is occurring in space. Radiation in space is far more active and challenging to model and test through the use of high energy particle accelerators. NASA

has the desire to test as they fly, which provided the opportunity to place coupons on the International Space Station(ISS) inside the pressurized volume as well as externally.

The environments provide two separate data sources for the study of composites exposed to radiation. The first being the study of composite coupons exposed to low doses of the radiation inside the pressurized volume of ISS in presence of oxygen. These coupons could also be used to determine if secondary particle showers due to high atomic number shielding have impact on the properties of the composites exposed to oxygen. There are studies that have been performed on other type of materials (CR-39 and Mica) which demonstrate that secondary particle impacts have occurred in these materials while in orbit. Figure 4 are images of the secondary impacts that created track marks on CR-39 detectors in which flown as experiments on ISS. These coupons had a lead foil between each detector. The presence of track marks increased substantially on the detectors that had the lead foils versus those that had no foil.

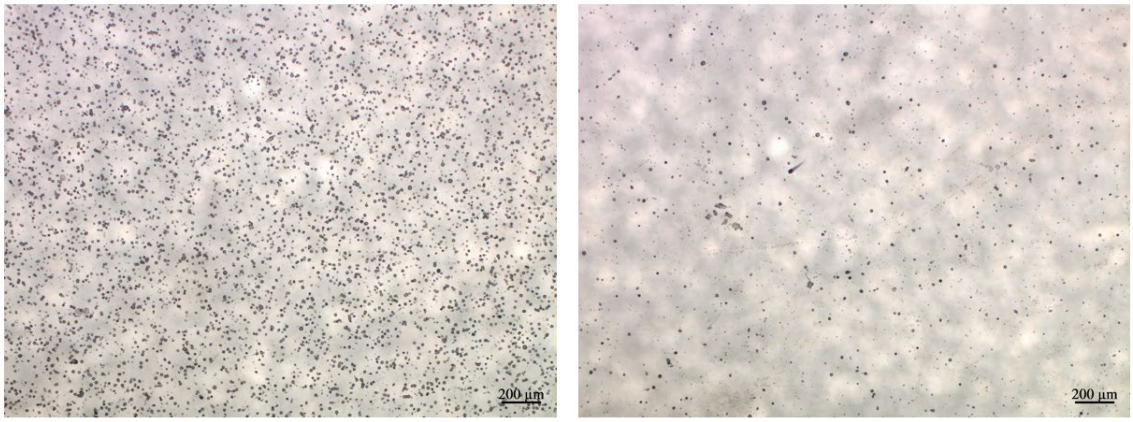

Figure 4: HiMassSEE CR-39 Coupon with Lead Foil (Left) and no metal foil (Right) after 924 days in orbit inside the pressurized volume of ISS

During the duration and time that the CR-39 coupons above were exposed to radiation on ISS, composite samples likewise were exposed in the same location on ISS. Based on the exhaustive review of other studies in which composites were exposed to radiation in an environment with oxygen, there is a desire to learn if secondary impacts due to high energy nuclear collisions between the protons and the composite materials nucleuses promote degradation such as cross-linking, chain scission and oxygen degradation.

The second portion of the study of interest is on coupons that are exposed outside of ISS and the impact that radiation has on unshielded composite coupons in a space environment. This review was originally desired due to being able to compare the degradation of the coupons between the interior and exterior of ISS. However due to the dimensional and quantity constraints on the coupons, that a direct comparison was not

possible in this study. There was still knowledge to be gained regardless of performing a comparison due to the absence of data from actual studies with radiation exposure in space.

CHAPTER II

METHODOLOGY

2.1 Composite Development

2.1.1 HiMassSEE Materials

In these experiments, composite panels were manufactured using the same process used for filament winding composite overwrapped pressure vessels (COPVs). The material selected was consistent with the most common aerospace COPV material, which is Toray T1000 carbon fiber. The epoxy matrix is proprietary to the company who manufactured the panels for the experiments. The composite panels were manufactured with a pre-preg fiber in which the fiber volume ratio was approximately 60%. The composite panels were tow wound on a flat panel mandrel (90-degree filament winding angle) so they could be cured and sectioned into smaller straight coupon specimens. The specimens were one tow thick to be consistent with the manufacturing plan for other strand specimens that were slated for stress rupture testing. The panels that were wound had peel ply placed on them to ensure a uniform straight specimen cross section during the oven cure process. The peel ply method is a process used to consolidate the overwrap in COPVs in industry and to ensure a uniform resin infusion process. The composite panels were then placed into the composite curing oven as witness specimens of COPV materials. They were cured along with COPVs that were stress rupture tested. The cure process consists of a ramp period in

which the composite was B-staged and then ramped up to the cure cycle temperature. The composite cure process has an eight-hour ramp and then held at 178°C or 350°F. The samples are then cooled down in three hours to ambient temperature (25°C or 72°F).

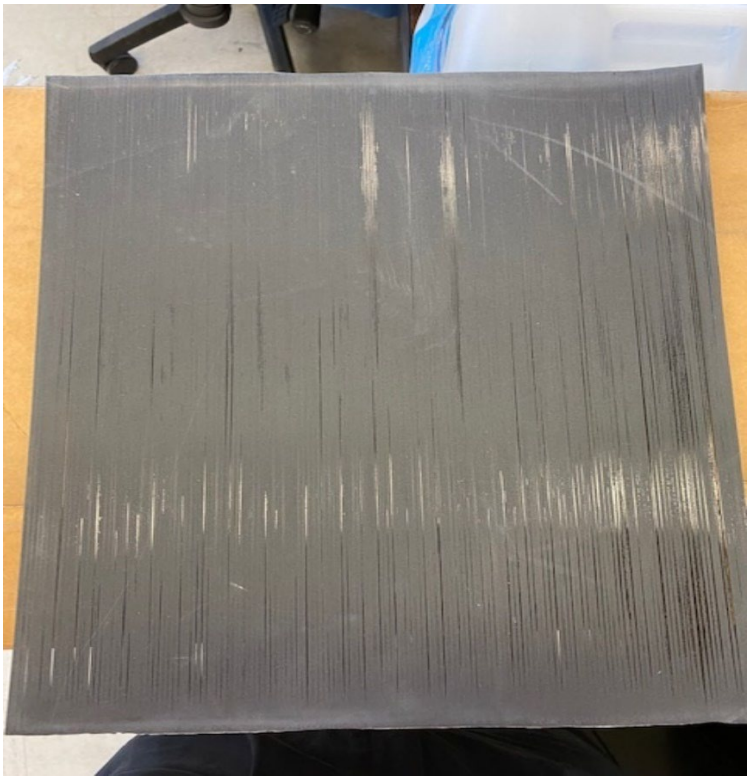

Figure 5: Post cure tow wound panel from the manufacturer of the HiMassSEE coupons

Once the panels were completely cured, they were removed from the oven. The peel ply was then stripped and prepared for separation from the mandrel. The panels were received at NASA Johnson Space Center (JSC) in Houston, Texas. Figure 5 above is a photo of the post cut panels. Note the matte finish of the panel due to the peel ply that was added at the end of the filament winding process (Figure 5). Upon closer inspection (using

2x magnification) imprinting of the peel ply is evident on the surface of as received specimen (Figure 5). This surface texture will be discussed in further detail in this document. Also, individual interfaces between individual 12k tows are evident as linear indications of "butt joints" as the peel ply compressed each adjacent tow together.

This contact of tows was not part of the baseline manufacturing plan. Rather, it was expected that each individual tow would be separated from adjacent strands. An individual strand cross section is well characterized from a strength and stress rupture perspective.

After completing the visual inspection of the composite panels, they were cut into smaller coupons for fitting into the radiation control boxes (also called "passive detector carriers"). These holders would house the coupons during launch and while in orbit during radiation exposure inside the ISS pressurized structure. Figure 6 is a coupon after cutting them in preparation for the ISS radiation exposure test. The coupon size is 2 x 4.7 x 0.5 centimeters. Table 1 below provides information about each composite coupon and how it was processed.

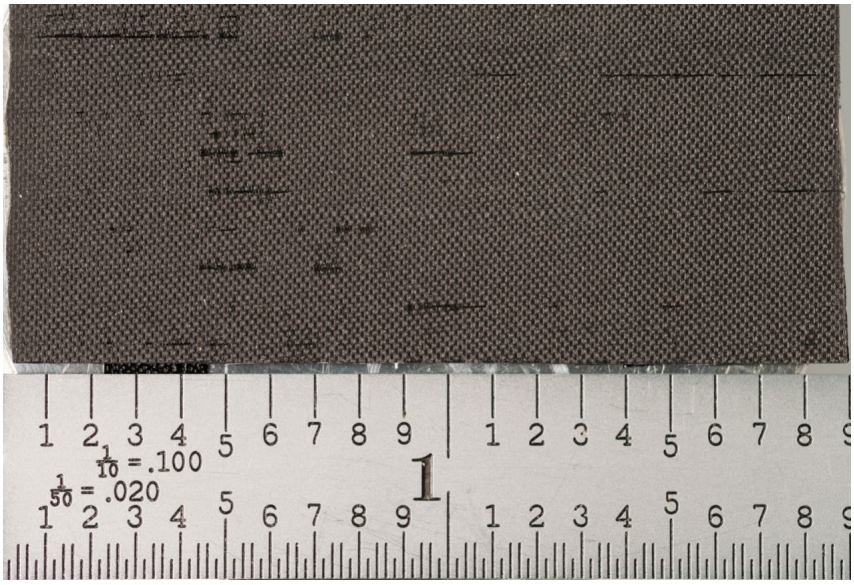

Figure 6: Composite Flight Coupon

These boxes were procured from Vanguard World and the original design of the box was to hold 8 RAM memory cards (figure 7). The boxes came with molded silicon liners that were removed and retro fitted with holders that fit the composite coupons. The boxes could carry up to 16 flat composite coupons in each box. The dimensions of the box are 6.2 x 10.2 x 1.5 centimeters, and the weight is 70 grams empty. The part number assigned to the box (SEY15550432-316) was used to track exposure of the specimens to radiation damage. Figure 8 shows the inside of the boxes prior to the removal of the silicone liner.

Figure 7: Exterior Image of the Passive Detector Carriers

Figure 8: Interior Image of the Passive Detector Carriers

Table 1: Composite Coupons Post Process Condition

Sample	Processed Condition
(CFCDET-1-1)	Cut to 2 x 4.7 x 0.05cm
(CFCDET-1-2)	Cut to 2 x 4.7 x 0.05cm
(CFCDET-1-3)	Cut to 2 x 4.7 x 0.05cm
(CFCDET-1-4)	Cut to 2 x 4.7 x 0.05cm
(CFCDET-2-1)	Cut to 2 x 4.7 x 0.05cm
(CFCDET-2-2)	Cut to 2 x 4.7 x 0.05cm
(CFCDET-2-3)	Cut to 2 x 4.7 x 0.05cm
(CFCDET-2-4)	Cut to 2 x 4.7 x 0.05cm
(CFCDET-3-1)	Cut to 2 x 4.7 x 0.05cm
(CFCDET-3-2)	Cut to 2 x 4.7 x 0.05cm
(CFCDET-3-3)	Cut to 2 x 4.7 x 0.05cm
(CFCDET-3-4)	Cut to 2 x 4.7 x 0.05cm
(CFCDET-4-1)	Cut to 2 x 4.7 x 0.05cm
(CFCDET-4-2)	Cut to 2 x 4.7 x 0.05cm
(CFCDET-4-3)	Cut to 2 x 4.7 x 0.05cm
(CFCDET-4-4)	Cut to 2 x 4.7 x 0.05cm
*All samples were precision cut in the NASA Materials and Processing Composite labs at JSC. After the coupons were cut, they were cleaned with IPA to ensure no composite dust was present on the coupons.	

2.1.1.1 Selection of the Foils

Heavy ion foils were selected for investigation similar to studies with CR-39 PNTDs. The thought is that secondary particle production resulting from collision of primary and secondary space radiation charged particles with a range of heavy metallic element foils interior to ISS will create track marks in the material. The foils consisted of Niobium, Tungsten and Lead. Table 2 below provides data on the material selected for the study.

Table 2: Material Foil Description

Material	Supplier	Part Number	Cut Size	Purity	Atomic number (Z)
Niobium (Nb) -Foil	Goodfellow	NB00-FL-000330	2.0cm x 4.7cm x 0.01cm	99.9%	41
Tungsten (W) - Foil	Goodfellow	W-00-FL-000240	2.0cm x 4.7cm x 0.05cm	99.95%	74
Lead (Pb) - Foil	Goodfellow	PB00-FL-000161	2.0cm x 4.7cm x 0.005cm	97.0%	82

The metallic foils were procured from Goodfellow, the material supplier used in in earlier NASA experiments on CR-39. The foil came in a roll in which was flattened and cut to the dimensions listed in Table 2. The foil was cut was in a controlled environment to ensure that containments and deposits (such as skin oil) was not in contact with the materials. Purity of the foil material was also a consideration in testing all materials (table

2). Purity was important for showing the effect of heaver versus lighter atomic number driven damage into specimens from the foils.

2.1.1.2 Assembly of the Track Detector Stack

The composite coupons and metal foils were cut to the required dimensions to fit into the aluminum passive detector carrier boxes. The coupons were placed into four stacks consistent with prior experiments that had flown on the ISS. The first of the stack was A-CFCDET-1, which contained the control coupons that had no metallic foil inserted between the composite samples. The second stack was A-CFCDET-2, with the Niobium foil placed between each composite coupon, the third stack was A-CFCDET-3, with the Tungsten foil placed between each composite coupon, while the final stack was A-CFCDET-4 coupons with the lead foil. Table 3 lists all the composite coupons of the assembled stacks. Figure 9 displays the stacking sequence used in every stack. The stacks were individually wrapped in a Permacel P-221 Kapton tape with acrylic adhesive. The thickness of the Kapton tape was 2.5 x 3 x 0.006 cm. The location of the aluminum passive detector carrier boxes with specimens was shown in Figure 8.

Table 3: Stack Assembly Material Map

Stack Assembly	Composite Coupon	Foil Material
A-CFCDET-1	(CFCDET-1-1)	No Foil (Control)
	(CFCDET-1-2)	
	(CFCDET-1-3)	
	(CFCDET-1-4)	
A-CFCDET-2	(CFCDET-2-1)	Niobium Foil
	(CFCDET-2-2)	
	(CFCDET-2-3)	
	(CFCDET-2-4)	
A-CFCDET-3	(CFCDET-3-1)	Tungsten Foil
	(CFCDET-3-2)	
	(CFCDET-3-3)	
	(CFCDET-3-4)	
A-CFCDET-4	(CFCDET-4-1)	Lead Foil
	(CFCDET-4-2)	
	(CFCDET-4-3)	
	(CFCDET-4-4)	

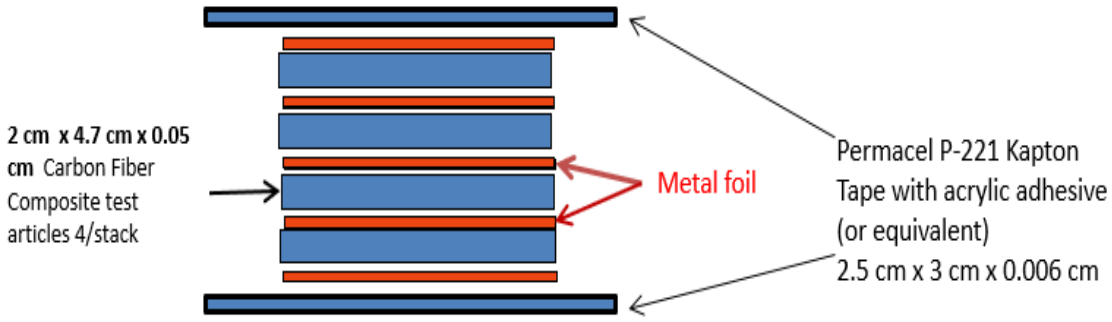

Figure 9: Assembly Stacking Sequence

After the stacks were placed in the mapped slots inside the aluminum passive detector carrier boxes, the boxes were shut and taped closed with Permacel P-221 Kapton Tape to ensure they would not open during launch or while on board ISS. SEY15550432-316 was packaged with group SEH29102950-304 and sealed in a flight poly bag. Flight was recorded before and after packaging. The weight of SEH29102950-304 prior to packaging was 307.0 grams and post packaging were 320.0grams. NASA JSC Materials and Processes lab (B13/RM258/260) balance (ID#M56489: 12Kg max) was used to measure the weights of each package. Figure 10 below shows the package group prior to being placed in the Nomex zero gravity storage locker. Figure 11 is an image of the SEH29102950-304 packaging placed in the Nomex zero gravity storage locker prior to close out.

Figure 10: Packaging Group SEH29102950-304 which contains SEY15550432-316

Figure 11: Packaging Group SEH29102950-304 prior to close out

2.1.2 MISSE-11 Materials

The MISSE-11 flight coupons were part of the Materials on ISS Experiments (MISSE) on the exterior of the International Space Station (ISS). They were a part of the NASA EPSCoR grant that Oklahoma State University (OSU) received (NNX14AN41A) titled "Radiation Smart Structures with H-rich Nano-structural Multifunctional Materials". New materials for future space flight missions are being developed and studied at OSU. One of the functions studied as part of the grant was focused on shielding from the radiation exposure that astronauts are exposed to while in space environments. "A major accomplishment of this project was the development of a carbon-fiber polyethylene composite that was called Space Composite 2020 or SC2020 for short. SC2020 comprised solely of elements which have the greatest inherent ability to shield space radiation, i.e., hydrogen, carbon, and oxygen. It also possesses both structural and material properties that make it highly suitable for use in the construction of pressurized tanks, e.g., for consumables like oxygen and water, and pressure vessels, e.g., the habitable volumes of spacecraft and planetary surface habitats." [16]

To maintain the structural integrity required, the SC2020 coupons were sandwiched between two carbon fiber/epoxy panels of 3mm think and 76.2mm x 76.2mm length and width. The SC2020 coupons and carbons fiber face sheets are shown in figure 12 below.

Figure 12: SC2020 Coupons Sandwiched with Carbon Fiber Coupons

"Absorbed dose from ionizing radiation was measured as a function of depth in each material using thermoluminescence detectors (TLDs) placed in wells of varying depth machined into the three materials. Analysis of the TLDs resulted in plots of absorbed dose as a function of shielding depth in the four materials, allowing for comparison of shielding efficacy the materials." [16]. For the MISSE-11 experiments, the driving purpose was to examine shielding and the absorbed radiation dose the coupons experienced. However, for the purpose of this study the carbon fiber/epoxy face sheets were studied in order to characterize the level of degradation that the coupons saw on the exterior of the pressurized volume of ISS. Table 4 below lists the different coupons that were used during the testing completed at Oklahoma State University in the Helmerich Research Center (HRC).

Table 4: MISSE-11 Carbon Fiber/Epoxy Face Sheets

Sample	Processed Condition
(CFRP(e) -1-1)	Cut to 76.2 x 76.2 x 3cm
(CFRP(e) -1-2)	Cut to 76.2 x 76.2 x 3cm
(CFRP(u) -1-1)	Cut to 76.2 x 76.2 x 3cm
(CFRP(u) -1-2)	Cut to 76.2 x 76.2 x 3cm
*All samples were cut in the Oklahoma State University HRC labs at OSU Tulsa. After the coupons were cut, they were cleaned with IPA to ensure no composite dust was present on the coupons. The subscript (e) refers to the flight coupons that were exposed to radiation and the subscript (u) refers to the ground controls that we not exposed to radiation.	

Figure 13 below shows the location where the TLDs were installed on the MISSE-11 experiments. Figure 14 below shows the SC2020 coupons with the radiation detectors loaded and taped with Kapton tape and secured in the corners post installation of the carbon face sheets.

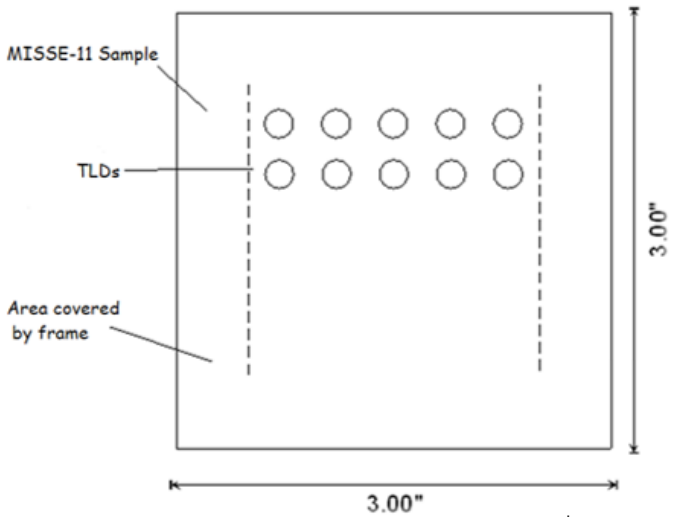

Figure 13: Diagram of PE-BN Sample Block with Detectors for MISSE-11

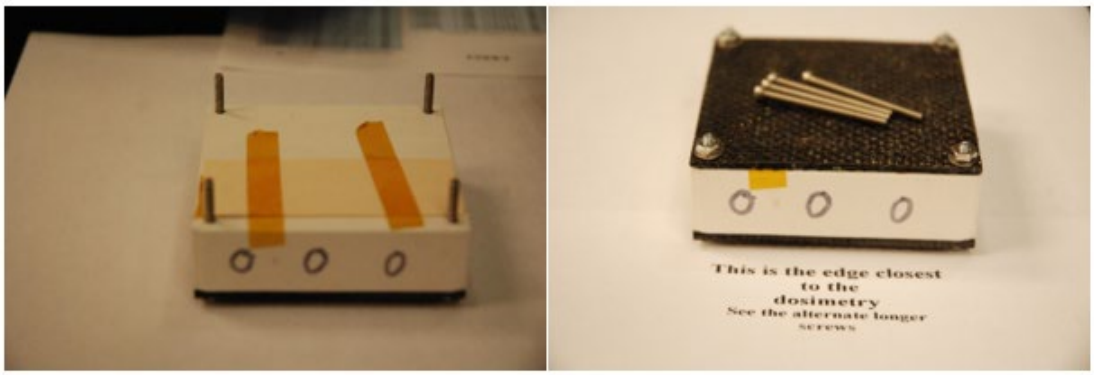

Figure 14: SC-2020 sample with radiation detectors loaded, without (left) and with (right) carbon composite cover in place.

"The sample blocks were secured to the MISSE tray, which was bolted to the MISSE experiment platform at NASA Langley Research Center to be included in the MISSE-9 and MISSE-11 experiments. The MISSE tray with the samples were prepared by Dr. Sheila Thibeault at NASA Langley Research Center." [2]

2.2 Characterization Testing

Characterization testing was limited by the constraints of packaging for flight exposure on ISS. The desire was to evaluate the effect of low earth orbit radiation on a composite strand material considering previously developed approaches. These tests consisted of scanning electron microscopy (SEM), tensile testing, dynamic mechanical analysis (DMA), differential scanning calorimetry (DSC) and Fourier transform infrared spectroscopy (FTIR). The tests were used to demonstrate changes in the composite material and mechanical properties due to secondary impact created by "high LET fission fragments and spallation products generated by thin metal foils exposed to the combined primary and secondary particulate internal to the ISS pressurized volume" [3, 4]. The testing was also used to determine changes in the material/mechanical properties of the MISSE-11 carbon/epoxy face sheets exposed on the exterior of the ISS pressurized volume. The following sections provide details on the methods and procedures used in this characterization process.

2.2.1 Mechanical Testing

The mechanical testing chose for testing the ground samples and the radiation exposed composite samples consisted of tensile tests and Dynamic Mechanical Analysis. The procedure for each was ASTM D2343 and ASTM D4062-12.

2.2.1.1 Tensile Testing

The tensile testing of the ground samples and radiation exposed were to follow the procedures outlined in ASTM D2343. The crosshead speed was selected at 1.27mm/min which has been used in previous tensile tests that involved radiation exposed coupons [6,7]. The area of radiation exposure was across the entire coupon which was equivalent to 940 mm^2. The area was calculated at 20 mm in width and 47 mm in length. The coupons were pre-cut, and the dimensions were controlled by the aluminum passive detector carrier boxes. Stress-strain data curves were to be generated from the data via an axial strain gauge that was attached the coupon. The following data was collected from the tensile pulls of the coupons: Modulus, ultimate strength, fracture strength, strain-to-failure, fracture energy, and first fracture point. Figure 15 below demonstrates graphically the collection of this data [6,7]

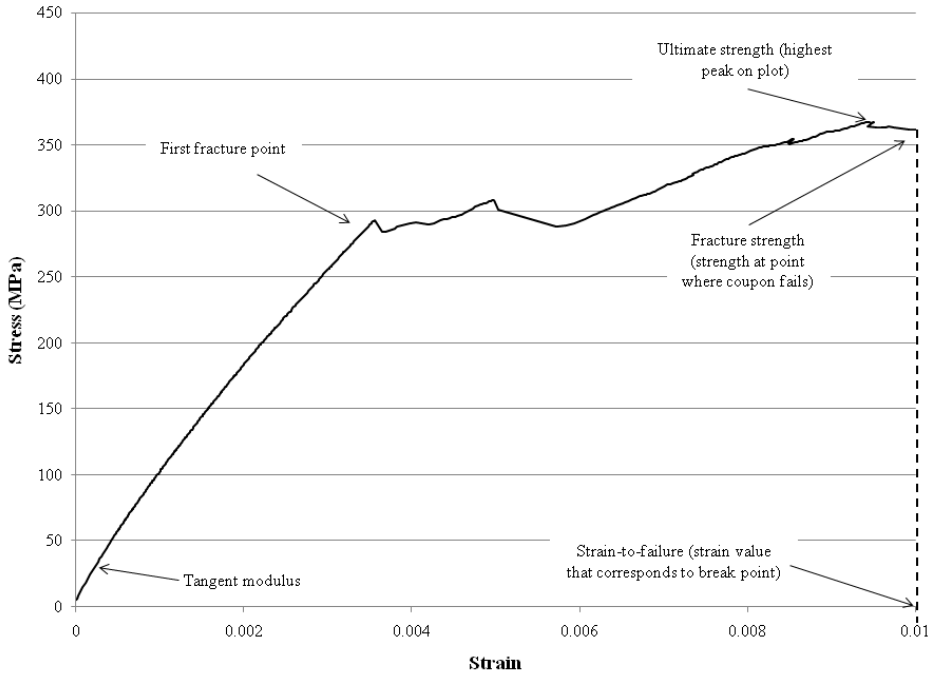

Figure 15: The graph above is representative of the stress-strain curve of a coupon that has been exposed to radiation and tensile tested

2.2.1.2 Dynamic Mechanical Analysis

Dynamic mechanical analysis (DMA) is the measurement of the mechanical properties of the materials as they are deformed under periodic stress. DMA provides insight in to how the storage modulus, loss of modulus, damping factor and the glass transition of the material could change as a function of the radiation exposure. ASTMD4062-12 was used as the documented procedure for performing the DMA. The instrumentation used was a DMA Q800 (TA Instruments, Inc., New Castle, DE). The specimens used for the DMA were SC2020 samples flown on MISSE-11 on the outside of ISS. Coupons were cut from the initial size of 76.2mm x 76.2mm down to a testing size of 57.9mm x 12.7mm x 2.29mm. The samples were then prepared and placed in a dual-

cantilever clamp with a span length of 35mm. Three-point bend tests were carried out by first equilibrating the coupons to 25°C and then heating the coupons from 30°C to 150°C at a ramp rate of 3°C/min and applying a constant stress load of 1N with 1 Hz frequency. The three-point bend test provides the storage modulus and the loss modulus. The dampening coefficient (tan δ) of the sample was measured using a Origin Pro 2022B analysis software. Figure 16 below demonstrates an example graphically the collection of DMA data results.

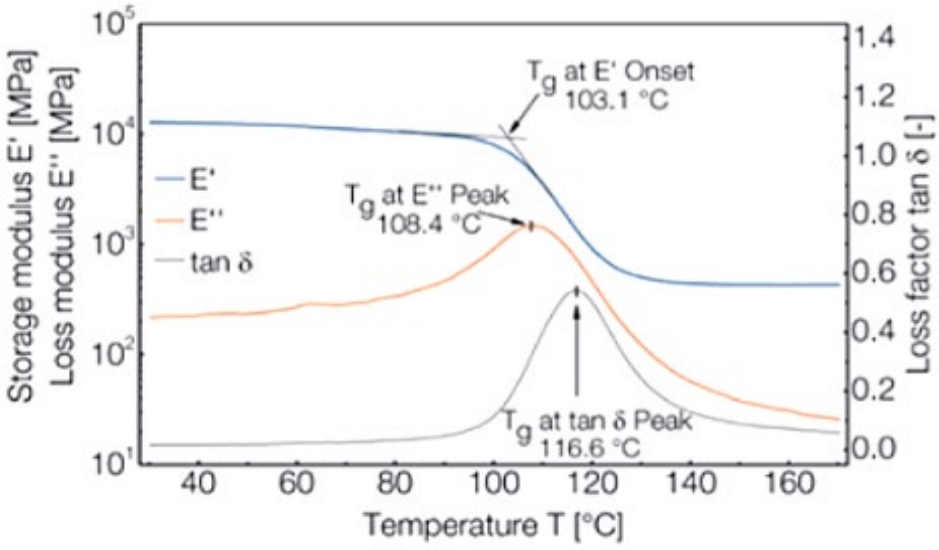

Figure 16: Example of a DMA data plotted on a Multiple Y plot

2.2.2 Differential Scanning Calorimetry (DSC)

Ground control coupons were cut to be representative of the flight coupons (2 x 4.7 x 0.05cm). The purpose for having the ground control coupons was to have a larger size coupon that could be used for fine tuning the testing parameters, due the limited flight

coupons that data could be collected from. The ground control coupons were stored in environmentally controlled areas and were not exposed to radiation. The second purpose of having ground controls was to be able to do a comparative study between ground controls, flight controls and layers foil stacks. The DSC test selected followed previous testing spectrum used on radiation exposed coupons the procedures using ASTM D3418-15. The experiments were performed using DSC Q2000 (TA Instruments, Inc., New Castle, DE). Table 4 below describes the parameters used. The purpose of performing DSC on the composite coupons was to determine if more cross-linking occurs post the manufactured curing cycle due to the radiation exposure.

Table 5: DSC Testing Parameters

Coupon	Equilibrate Temp	Ramp 1	Ramp 2	Ramp 3
Ground Control (TBD)	-50 C	50 C/min to 250 C/min	25 C/min to -50 C/min	50 C/min to 250 C/min
Flight control (CFCDET-1)	-50 C	50 C/min to 250 C/min	25 C/min to -50 C/min	50 C/min to 250 C/min
Nb Foil coupon (CFCDET-2)	-50 C	50 C/min to 250 C/min	25 C/min to -50 C/min	50 C/min to 250 C/min
W Foil Coupon (CFCDET-3)	-50 C	50 C/min to 250 C/min	25 C/min to -50 C/min	50 C/min to 250 C/min
Pb Foil Coupon (CFCDET-4)	-50 C	50 C/min to 250 C/min	25 C/min to -50 C/min	50 C/min to 250 C/min

2.2.3 Scanning Electron Microscopy (SEM)

2.2.3.1 HiMassSEE SEM Images

Examination of the coupons under the scanning electron microscopy (SEM) was completed on the ground controls, flight controls and foil stacked coupons. The purpose for performing SEM on the coupons was to determine if track marks were visible. In previous experiments, even though track marks were seen on exposed CR-39 detectors, they were not visible under the SEM and had to be etched to in order to open the pore sizes and identify them. Another area of interest was to examine whether there was degradation to the epoxy in which exposed fibers were breaking through the epoxy which would demonstrate weaking of the matrix. Unfortunately, due to the cross section of the coupons, depth of penetration could not able to be detected effectively.

2.2.3.2 MISSE-11 SEM Images

Examination of the coupons under the scanning electron microscopy (SEM) was completed on the ground controls and flight controls coupons. The purpose of performing SEM on the coupons was to determine if there were high energy particle impacts that created track marks on the flight coupons on the exterior of ISS. Another area of interest was to examine whether there was degradation to the epoxy in which exposed fibers were breaking through the epoxy which would demonstrate weaking of the matrix. Due to the lack of a sufficient quantity of coupons, destructive evaluation such as cross section could not be performed. These coupons were also needed for DMA testing.

2.2.4 Fourier transform infrared Spectroscopy (FTIR)

The HiMassSEE carbon coupons were examined using Fourier transform Infrared Spectroscopy (FTIR) to better understand the material from a molecular level and to better investigate which chemical bonds have changed with the irradiation. The FTIR experiments were run using the Attenuated Total Reflectance (ATR) method. A Shimadzu IRSpirit with QATR-S having diamond prism was used for attenuated total reflection FTIR (ATR-FTIR). The spectra were collected by acquiring 16 scans at a resolution of 2 cm-1 in absorbance mode ranging from 500 to 4000 cm-1. The ATR method allows for investigation of the surface. Prior to characterizing any panels, a background spectrum was obtained and subtracted from the subsequent sample spectra. This process enabled the removal of any background noise, such as water, from the signal so that weaker signals could be more easily observed. Pressure was applied during data collection to ensure that there was adequate contact between the sample and the ATR crystal. Figure 17 is a sample FTIR (ATR) of an irradiated carbon fiber/epoxy composite sample.

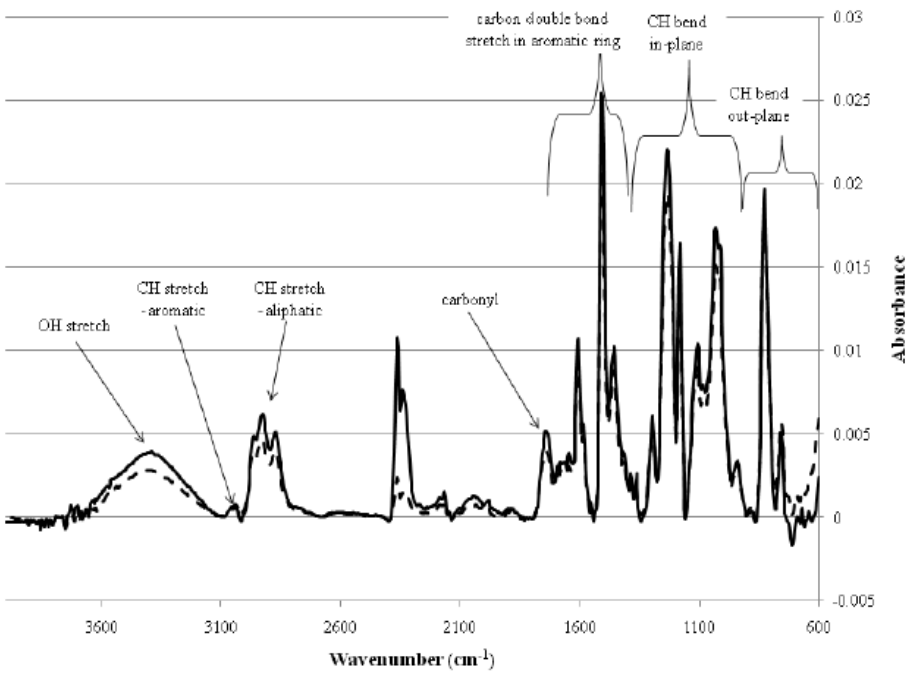

Figure 17: Carbon Fiber/Epoxy irradiated coupons tested by FTIR (ATC)

2.3 Radiation Testing

2.3.1 Materials on the International Space Station (ISS) HiMassSEE Kit 4 Sample set SEY15550432-316

The composite coupons were launched out of NASA Kennedy Space Center and delivered to the International Space Station (ISS) for 2 years, 6 months and 11days. The coupons were located inside of the ISS pressurized volume in the US LAB ZRS Locker. Figure 18 below is a diagram of ISS and circled in red was the location of where the coupon specimens were kept. Figure 19 is a photo of the HiMassSEE flight kits floating in zero gravity onboard ISS. The range of shielding mass thickness for the US LAB on ISS is 20 to 50 g/cm^2. Based on the SSP-30512 Design/Verification Environment requirements for

the US LAB the annual does estimates range from 8 cGy to 21 cGy with a median value of 14 cGy depending on the location of the dose point [4].

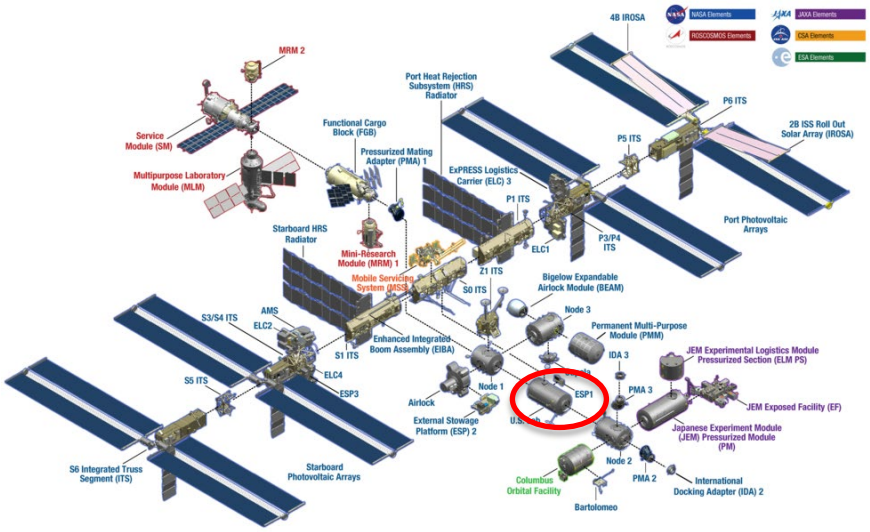

Figure 18: ISS Diaphragm and location of the Composite Coupon Specimens

Figure 19: Composite Coupons onboard ISS Materials on the International Space Station (ISS) MISSE-11 Experiment

"The MISSE-11 experiment was launched to the ISS aboard the NG-11 launch vehicle on 17 April 2019. The MISSE-11 experiment was deployed aboard ISS on May 2, 2019 and was scheduled to be exposed to the radiation environment external to the ISS for approximately one year. However, the MISSE-11 was returned to the ground on April 9 2020 and received by the laboratory at OSU on April 28 2020. The date the MISSE-11 experiment was retrieved from outside ISS is not known and hence the total duration of the external exposure is unknown." [16]

MISSE-11, which was similar to a prior MISSE-9 experiment was located outside of the pressurized environment of the International Space Station. The coupons were placed in the Zenith orientation. This is shown in figure 20(a) below. "This position has the highest solar exposure and a grazing atomic oxygen (AO) exposure. The location of the PE-BN and PE-BC samples for MISSE-9 can be seen in figure 20b). For MISSE-11, the samples were in the same location." [2]

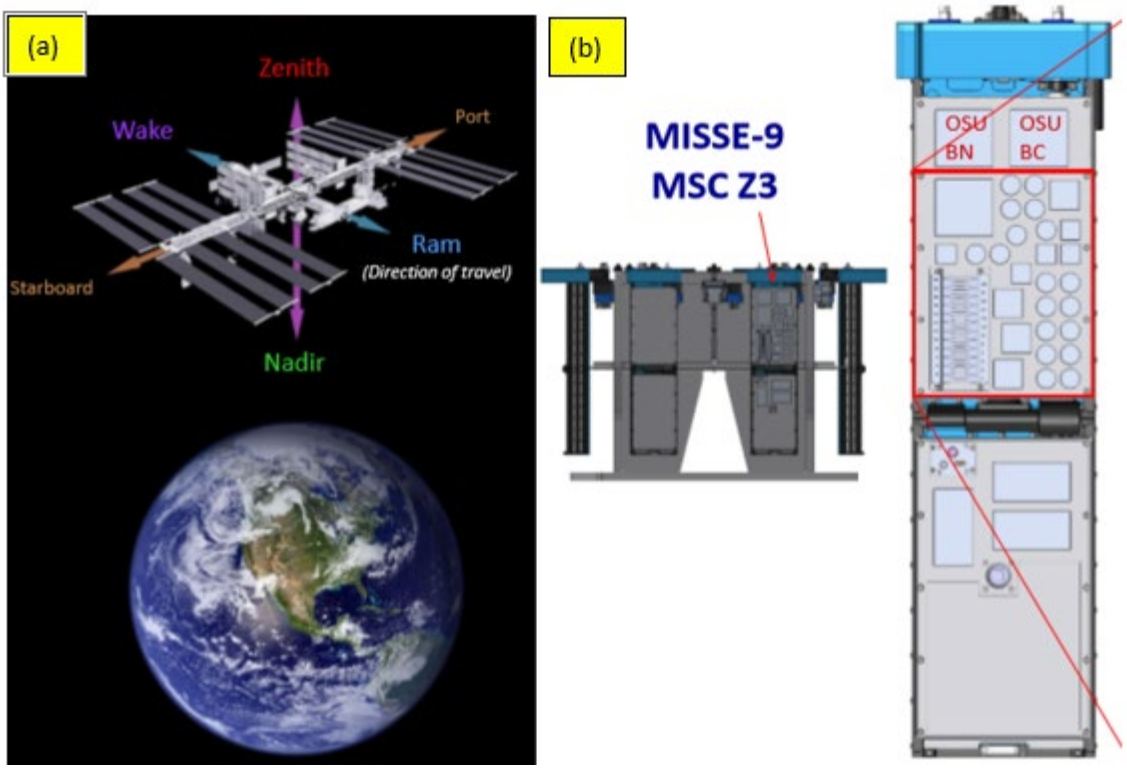

Figure 20: MISSE Sample Locations: (a) Flight Orientation and (b) Module Location

CHAPTER III

RESULTS

3.1 Characterization Tests

3.1.1 Mechanical Testing

3.1.1.1 Tensile Testing

The mechanical testing that was selected for determining the impact of the radiation had on the composite coupon specimens was tensile testing. The tests were to be used to characterize the material properties and compare them to each other. Once the composite coupons were delivered to JSC for processing and pretesting setup it was determined that there was an issue with the test coupons that was not originally considered. Due to the manufacturing and peel ply applied to the fiber, the individual tows cured together. This provided immediate concerns that when separating the tows apart there would be damage that occurred to the edge of the tow that would more greatly impact the material properties that would result in a false testing showing degradation of strength when in fact it was the processing error that would have created this degradation. Figure 21 demonstrate the issues that arose when trying to separate the fiber tows from each other.

Figure 21: Composite Coupon that was separated from group of tows. Signs of fiber tearing occurring from the separation

The next issues that arose from the review was that the composite coupons themselves were way too small to fit into standard load frames. Alternative methods of tensile testing have been developed by NASA White Sands Test Facility in Los Cruses, New Mexico for small strand testing. The process involved tabbing the strands with cardboard strands as shown in Figure 22 and testing the strands in a micro-load frame that was developed previously for testing Kevlar 49 roving in the SEM. Figure 23 is a picture of the micro-load frame. Unfortunately, constraints on the size of the specimens meant that ASTM D2343 could not be used to generate tabbed strand specimens as had been done in the work of [17, 18]. Collaboration with NASA White Sands Test Facility into the possibility of using a micro-load frame also turned out to be problematic due to the short gauge length of the specimen and the fact that the strands were joined to each other and would not fit the width constraint of the instrument.

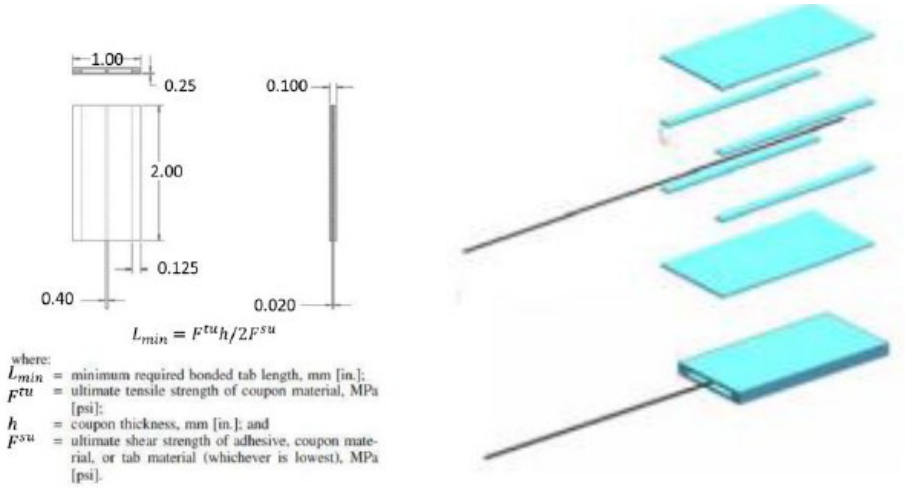

Figure 22: Cardboard tabbing of carbon fiber strands

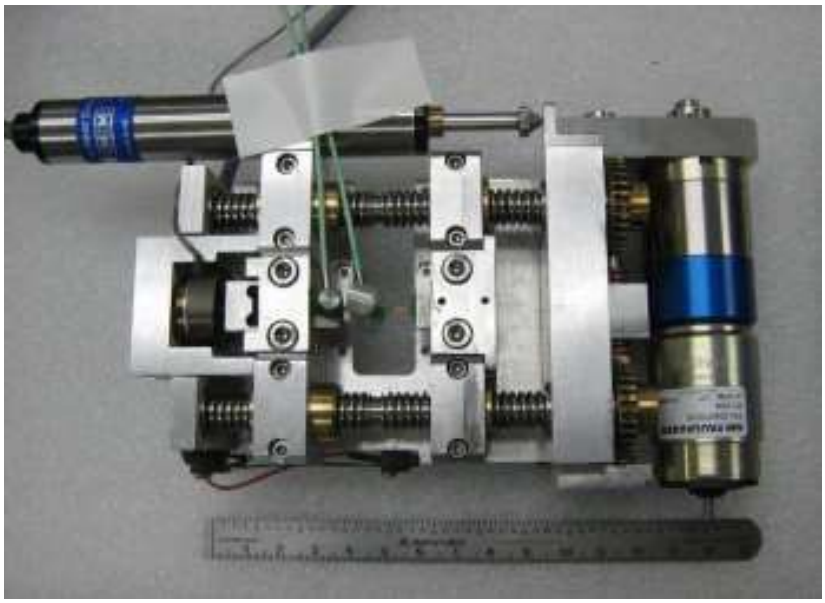

Figure 23: Micro Load Frame

3.1.1.2 Dynamic Mechanical Analysis

DMA was used to examine the effect of temperature on the storage modulus (E') and the loss modulus (E") on the carbon fiber/epoxy face sheet coupons from the MISSE-11 experiments. Due to the size constraints of the HiMassSEE coupons, DMA could not

be used to test these coupons. The CF/Epoxy face sheet coupons from the MISSE-11 experiments were supposed to be irradiated on exterior of ISS for one year; however based on when the coupons were launched and returned to the surface, the exact time of exposure was unknown. Regardless of the period of exposure there was still knowledge and data that was learned and gathered through DMA on the flight specimens and ground controls that were made.

It was observed that as the temperature increased, the storage modulus decreased around 50°C. Figure 24 shows that the storage modulus of all the 4 samples decreased as the temperature increased. Figure 25 is a comparison of the irradiated and the ground specimens. It can be observed that no significant change between the irradiated and ground specimens. Figure 26 displays the loss modulus as temperature increased individually plotted for all coupons, while Figure 27 is the comparison of the loss modulus for all the samples. Damping factor, or tanδ was also recorded to see if there was a difference between the ground controls and the flight coupons. Figure 28 and Figure 29 display the individual coupons results and the comparative results.

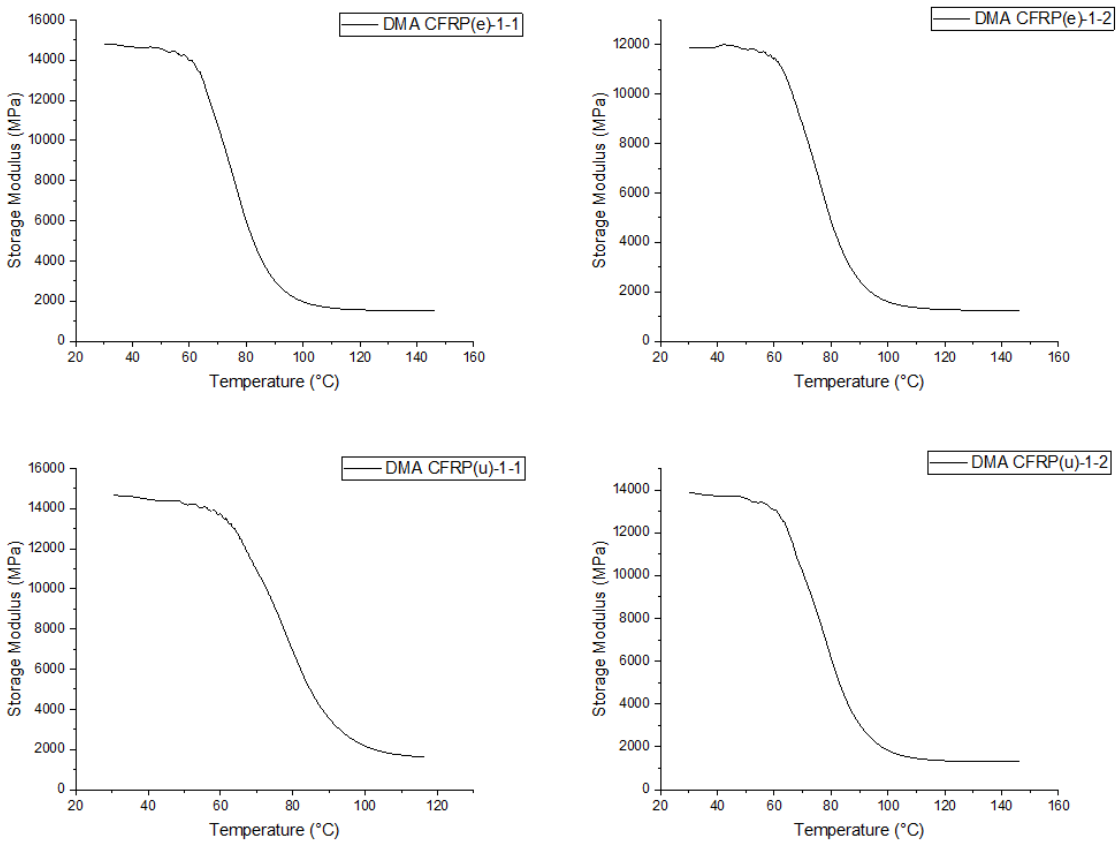

Figure 24: Plot of the Storage Modulus vs. Temperature of flight vs. ground control

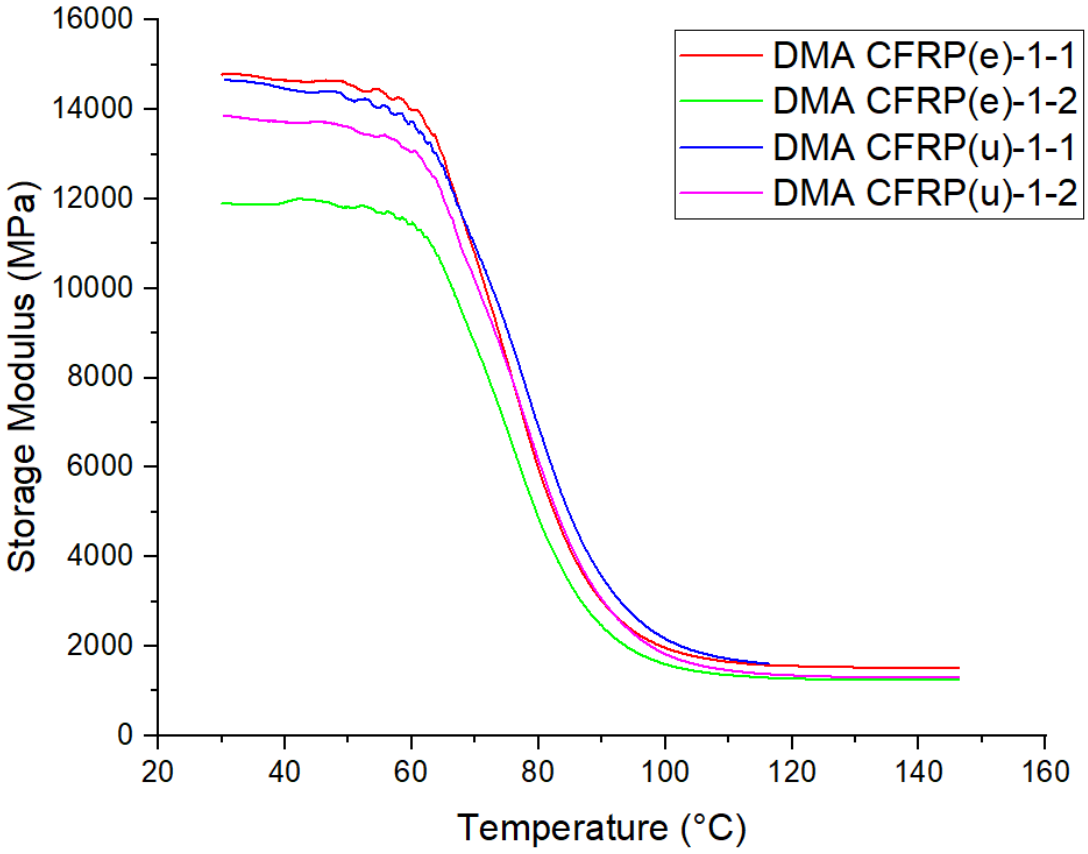

Figure 25: Plot of the Storage Modulus vs. Temperature comparison of flight vs. ground control

Figure 25 above shows that there are minor changes in the storage modulus between CFRP(e)-1-1, CFRP (u)-1-1 and CFRP (u)-1-2. The DMA data for CFRP (e)-1-2 however shows that there is a reduction in the storage modulus. The difference between DMA CFRP (e)-1-1 and DMA CFRP (e)-1-2 is 2883 MPA. Both these coupons were irradiated outside the ISS , but only one of the coupons (CFRP (e)-1-1) showed no change from the ground controls. The reduction of storage modulus could be attributed to CFRP (e)-1-2 receiving higher doses of atomic oxygen due to its orentiation.

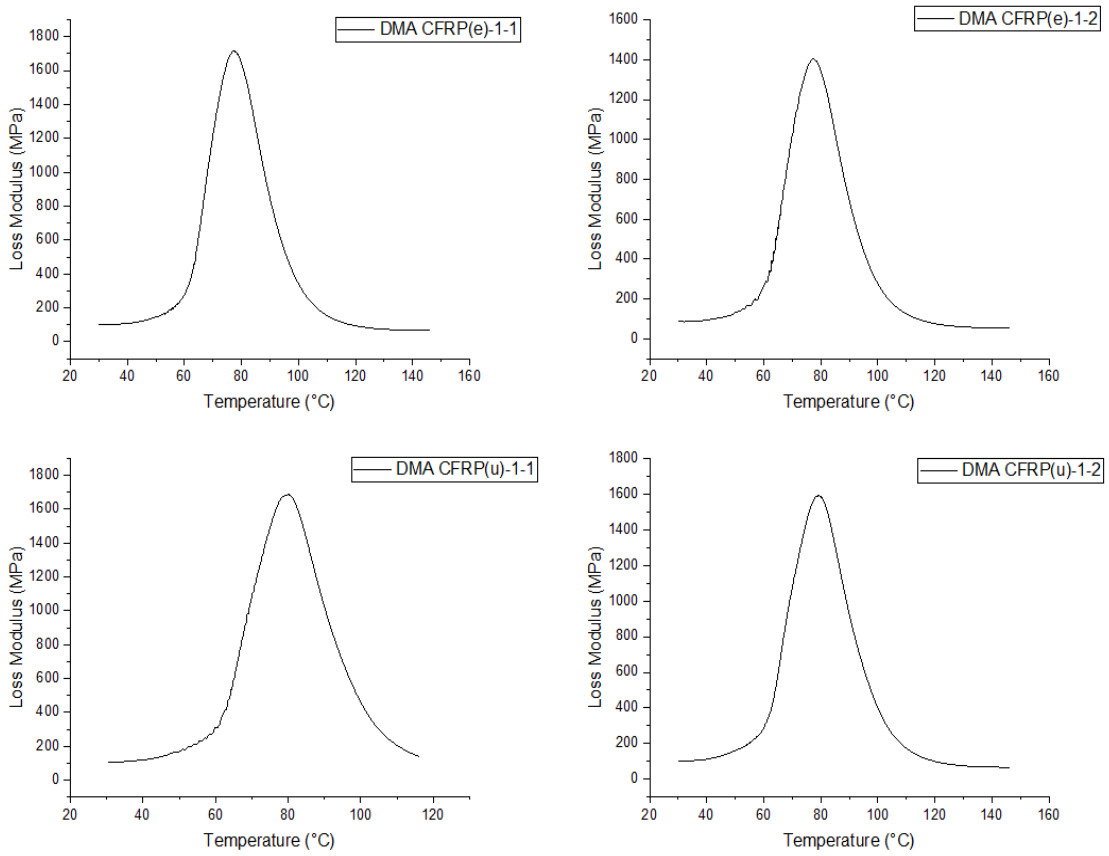

Figure 26: Plot of the Storage Modulus vs. Temperature of flight vs. ground control

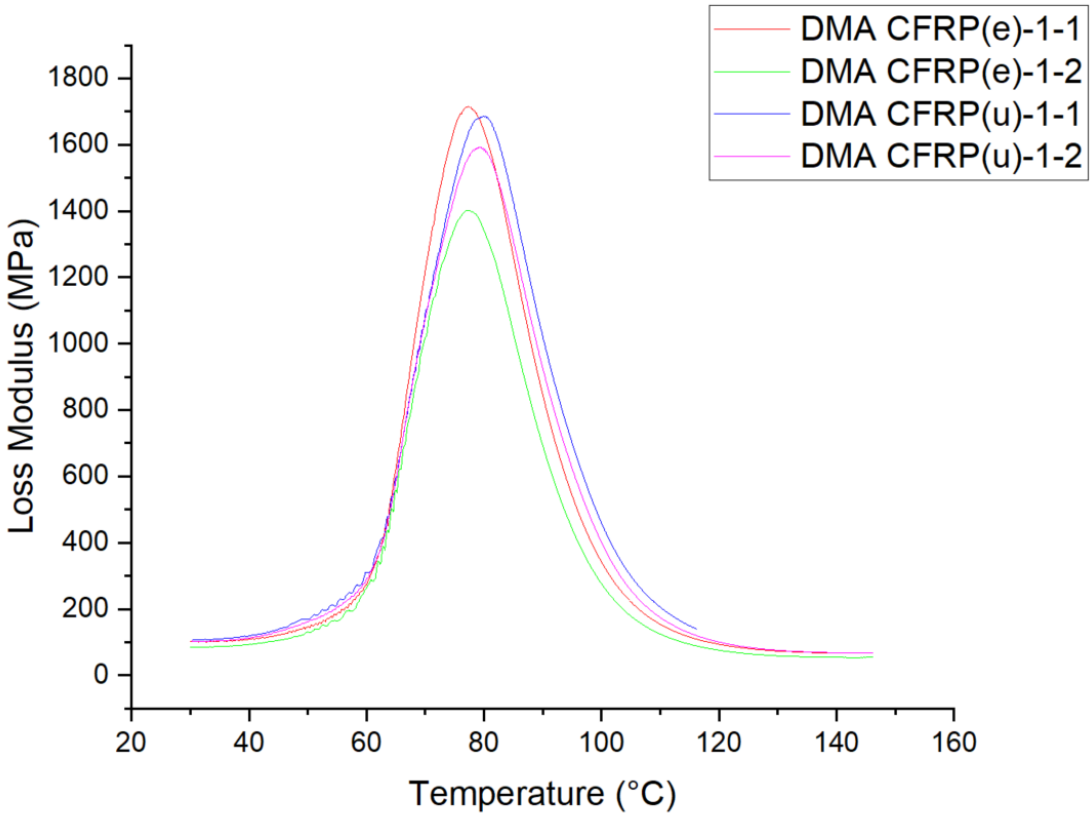

Figure 27: Plot of the Loss Modulus vs. Temperature comparison of flight vs. ground control

Figure 27 above demonstrates that CFRP (e)-1-2 has undergone a change in which the molecular motion in the epoxy has become more pliable or softened. This is typical of irradiated composites. Similar to figure 25, there is a noticeable difference between the irradiated coupons CFRP (e)-1-2 and CFRP (e)-1-1 which tends to follow similar pattern of the ground control samples. The only difference again between these coupons would be the location and direction of the coupons on the outside of ISS, which could have resulted in a difference in the radiation doses.

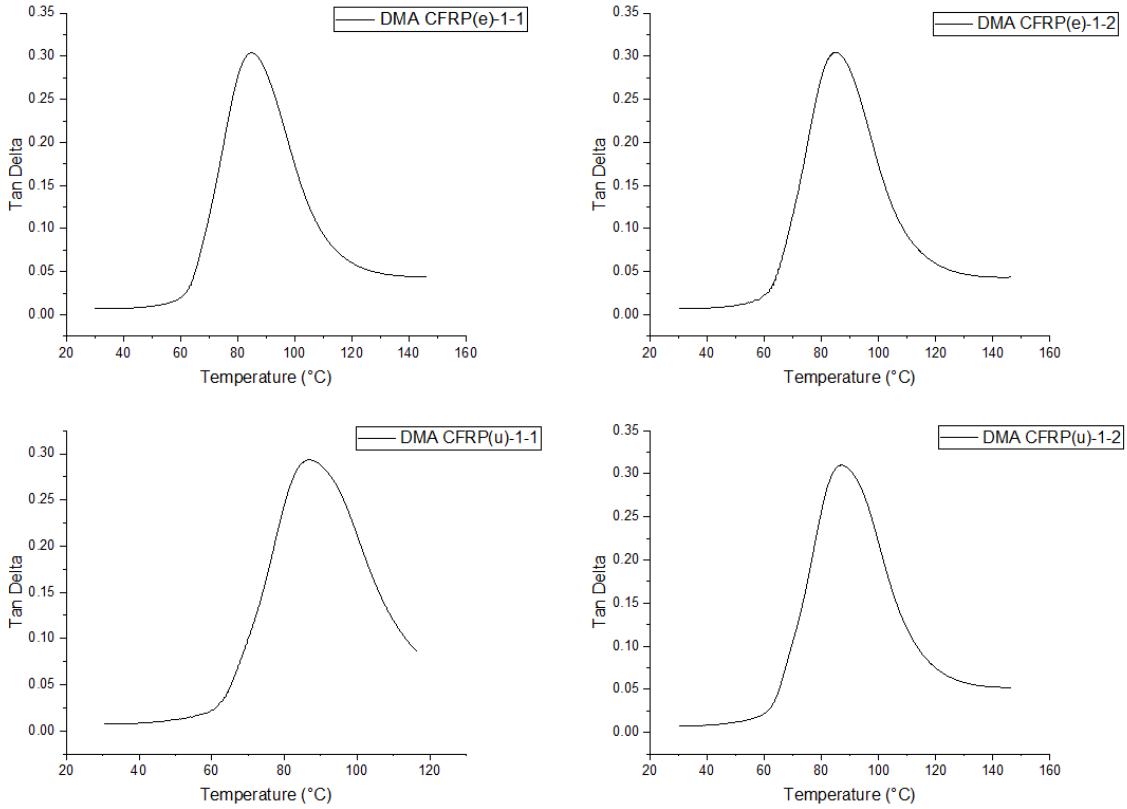

Figure 28: Individual damping factors of each of the MISSE-11 coupons

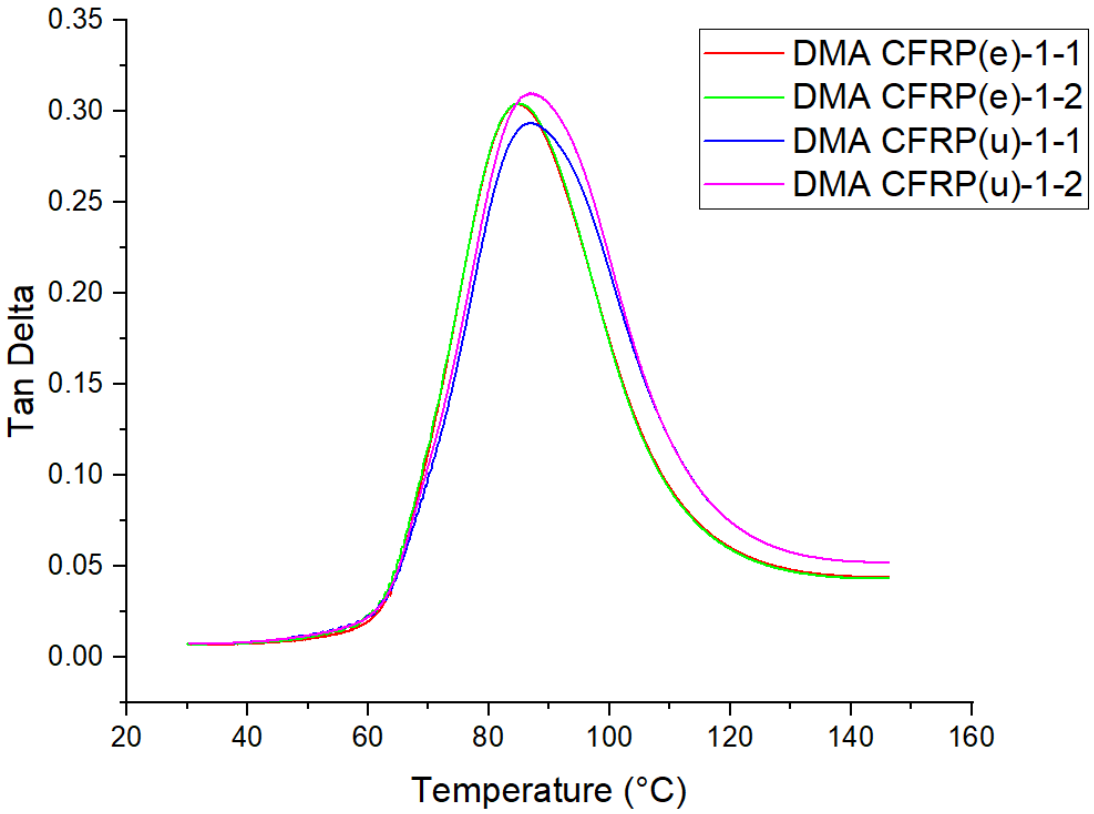

Figure 29: Comparative plot of Delta Tan on MISSE-11 coupons

The damping factor or Tan Delta data demonstrated that the molecular structure and mechanical properties were affected as the temperature was increased. Both the irradiated samples showed a slightly higher tan delta, which is indicative of an increased molecular weight versus a broader peak of the ground controls which could be attributed to a larger distribution of molecular weights.

Figure 30 below provides information needed to calculate the glass transition temperature of each of the coupons. The glass transitions demonstrate the while there is little difference between the ground controls and the flight coupons there is still a slight difference which would be attributed to the environments in which the coupons were located.

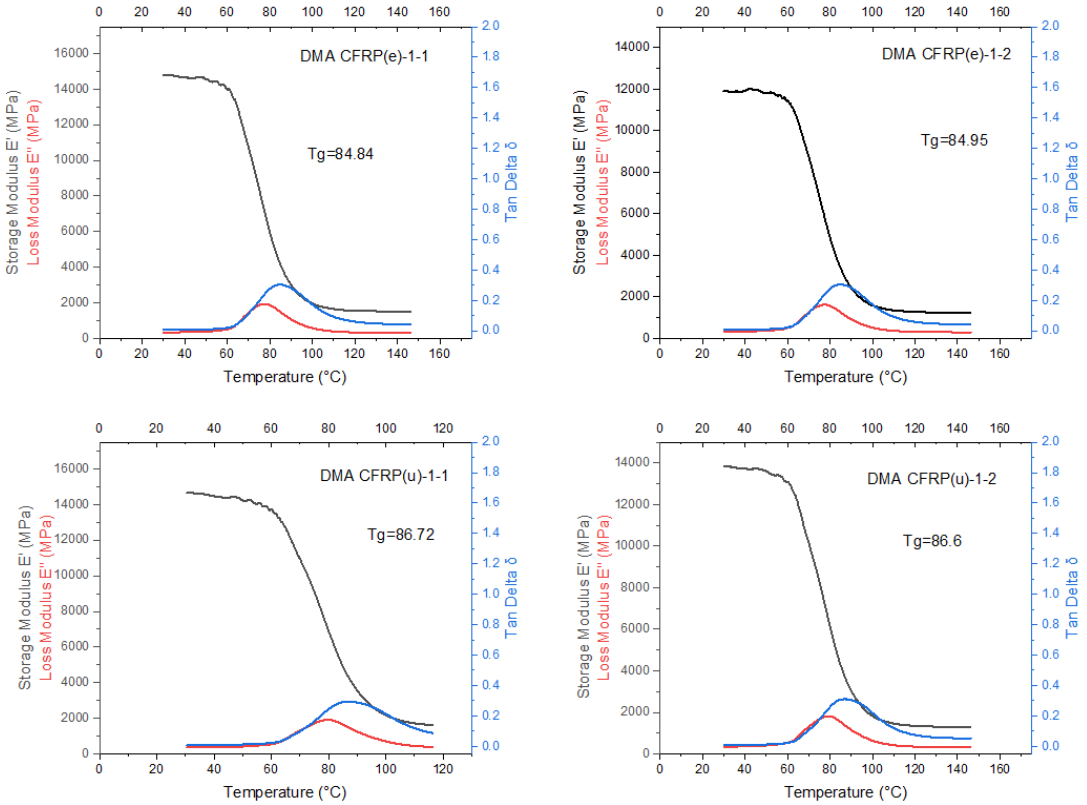

Figure 30: Plotted Storage Modulus, Loss Modulus and Tank Delta with determined glass transition temperature of the flight and ground control coupons for the MISSE-11 experiments

3.1.2 Differential Scanning Calorimetry (DSC)

DSC was used for determining the glass transition (Tg) and the recrystallization point of the HiMassSEE coupons. The MISSE-11 coupons were not a part of this testing regime due to the lack of quantity of coupons that were present for running experiments. Examination of the glass transition and recrystallization state of the coupons will find in determining the chemical state of the coupons and whether cross-linking or chain scission is occurring more on the ground controls vs. that of the flight coupons. "Decreasing T_g values with radiation exposure indicates that chain scission increases with increased radiation dose. Similar effects were reported in, and one report concluded that scission predominates when the material is fully cross-linked. The lack of any cure peaks in the

DSC data indicates that the samples were fully cross-linked before radiation. Thus, chain scission in the epoxy is expected with increased radiation exposure." [6, 7, 19, 20]

"Furthermore, previous work has shown an empirical correlation between T_g and the degree of cross-linking.

$$M_c = (3.9x10^4) / (T_g - T_{g0})$$

In this equation M_c is the number average molecular weight between cross-links, T_g is the glass transition temperature, and T_{g0} is the glass transition temperature of the pre-cured epoxy. As the glass transition temperature decreases, the molecular weight between cross-links increase, indicating a degradation of the epoxy network structure." [6, 21, 22, 24, 23].

The plotted data shown in Figure 32, shows that there are no cure peaks that occur in the coupons in the first heat cycle, which could demonstrate that all the coupons were fully cross linked prior to being irradiated as there is not a major difference shown between the ground controls and the flight coupons. Figure 31 is the comparison of the all the coupons, while once again there is no noticeable curing peaks found. There is a difference in slope from that of the ground control coupons which does suggest that the irradiated coupons could be undergoing chain scission.

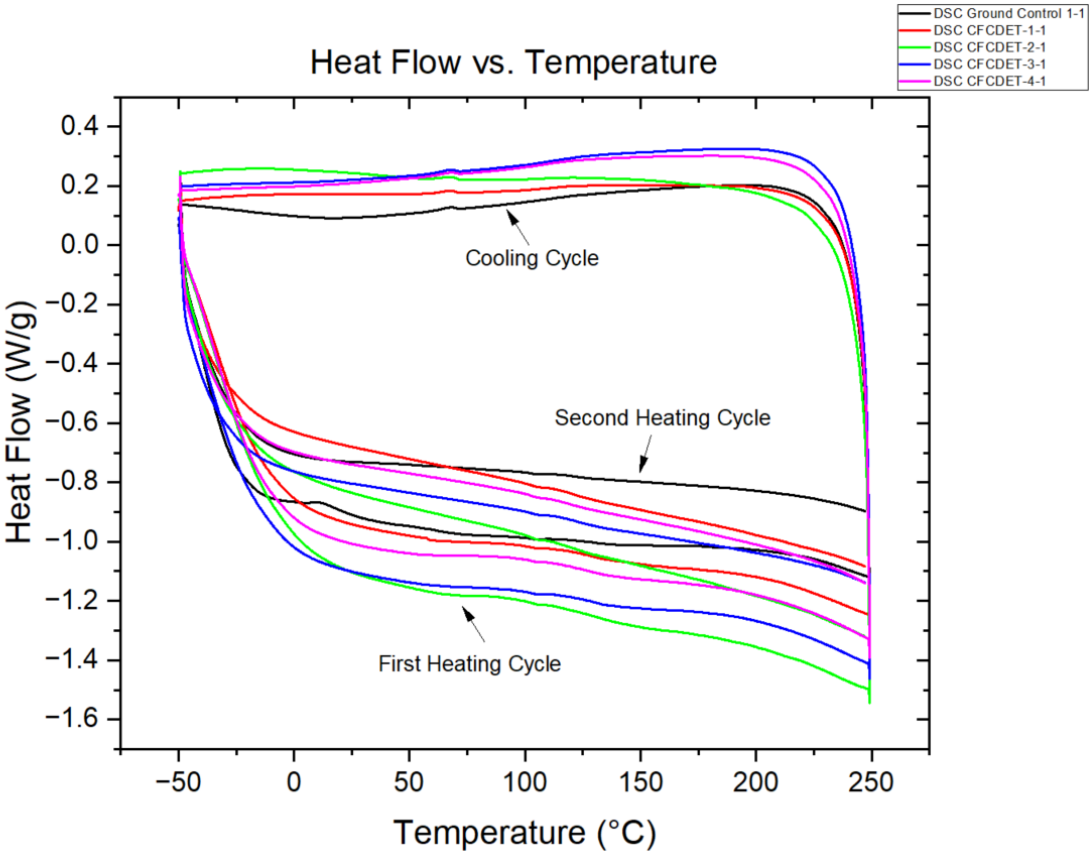

Figure 31: Comparison data plots of HiMassSEE coupons (ground controls and Flight coupons)

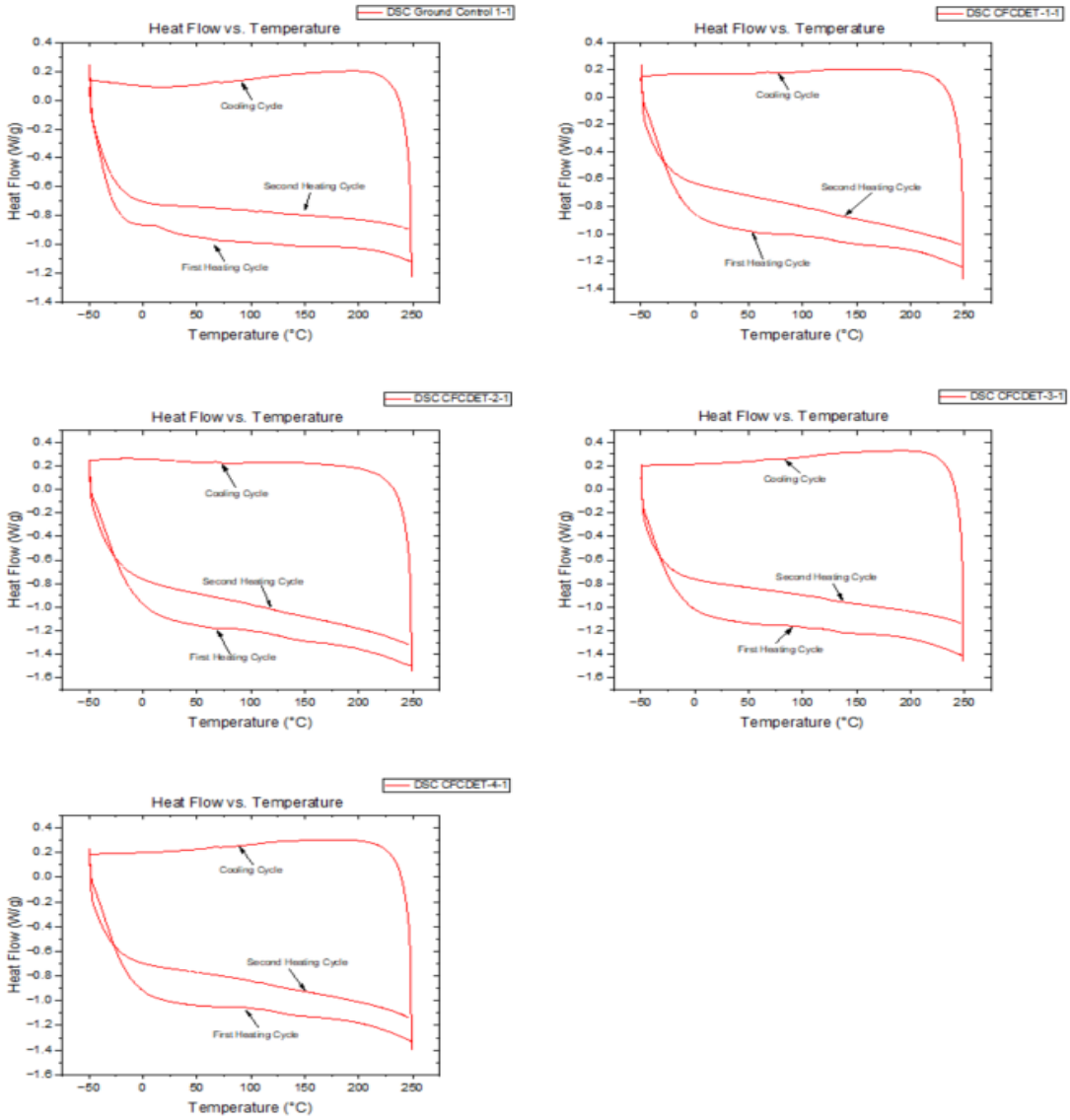

Figure 32: DSC Heat Flow vs. Temperature Results for the Heating and Cooling cycles performed on the HiMassSEE Carbon Fiber/Epoxy Coupons

3.1.3 Fourier Transform Infrared Spectroscopy (FTIR) Analysis Testing

FTIR was used for to determine if there was a change in the coupons after being irradiated. The HiMassSEE coupons were used in these experiments due to the lack of having enough MISSE-11 coupons. Five coupons were studied to determine the difference in the peaks between the ground controls and the flight coupons. In general, with radiation exposure, several absorbance peaks increased when compared with ground control coupon

values. However, one of the flight coupons (CFCDET-2-1), experienced less absorbance than ground control coupons which was not exposed to any radiation. In the region of 1750 cm^{-1} to 2250 cm^{-1} there are peaks with lower absorbance peaks in the data (Figure 33), which could be representative of oxidation. Figure 34 is the FTIR test results of all the samples.

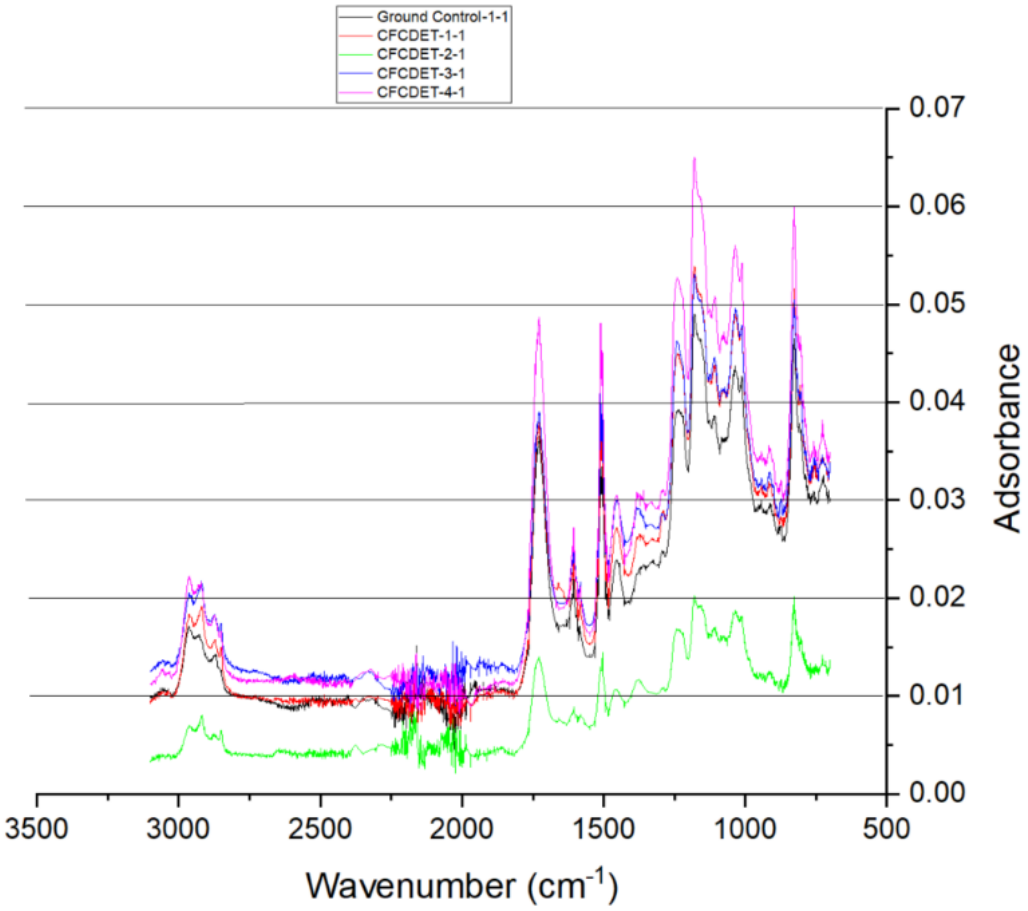

Figure 33: FTIR Comparison data plots for the HiMassSEE Coupons

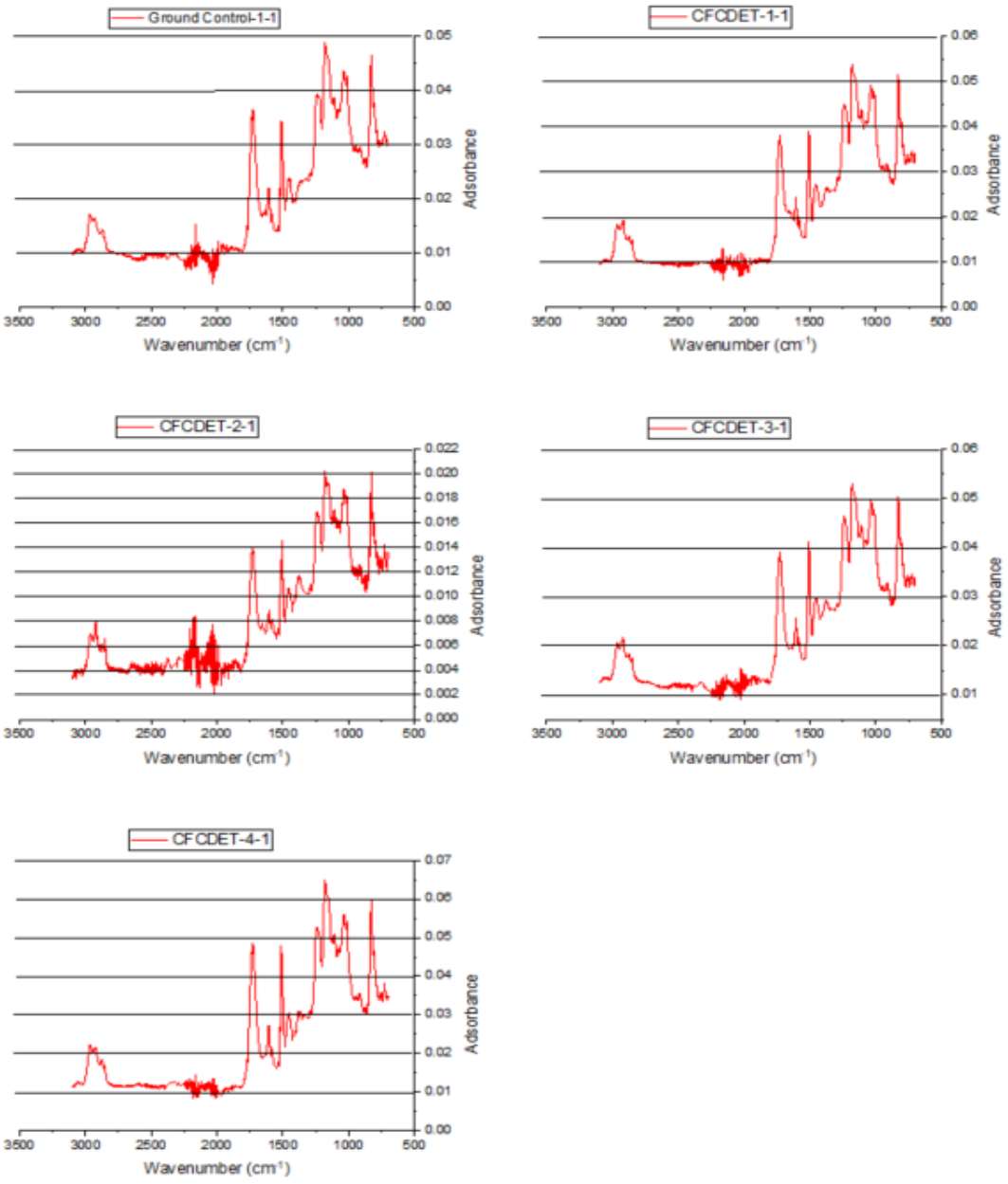

Figure 34: FTIR Test Data Plots of the HiMassSEE Coupons

3.1.4 Scanning Electron Microscope (SEM)

3.1.4.1 HiMassSEE Results

Prior to completing any testing on the HiMassSEE coupons SEM was conducted to characterize the surface condition of the coupons. In these images the focus was to

determine if there were any noticeable track marks that could be related to secondary particle impacts due to the foil shielding. SEM was also of interest to investigate whether the fibers were fully covered by the matrix (epoxy) which could be indicative of strong adhesion between the carbon fibers and the matrix. A change in the adherence of resin to the fiber surface could indicate a weakened fiber-matrix interface bond because of the irradiation exposure [6,7]. All coupons were compared with the ground control samples. The flight coupons were likewise compared to each other due to the hypothesis that higher the atomic number of the metal foils, higher the degradation of the surface. Each of the coupons were examined at different positions, magnification, and resolution. Figures 35, 36, 37, 38 and 39 are SEM images of the ground control coupon, flight controls (Non foil), flight coupon with Niobium foils (Nb), flight coupons with Tungsten (W) foils and flight coupons with Lead (Pb) foils.

Figures 40, 41, 42, 43 and 44 are comparisons of the ground controls and flight coupons and the flight coupons compared to each other. Based on the results, the various images indicate strong adhesion between the carbon fibers and the matrix. In Figure 44, no significant change is seen in the interface between the carbon fibers and the matrix. Thus, the interface of the CF material did not get affected because of radiation exposure inside the ISS. The peel ply that was added during manufacturing created a very distinct cross hatch pattern on the surface of the coupons which added to the difficultly in identifying areas in which there were expose fibers. There is also a difficulty in determining any track marks left by secondary impacts due to the carbon fiber being non-transparent as past experiments with Mica and CR-39 detectors were. Even with those experiments, chemical

etching was required to expose the track marks for examination with high powered microscopes vs. the use of SEM.

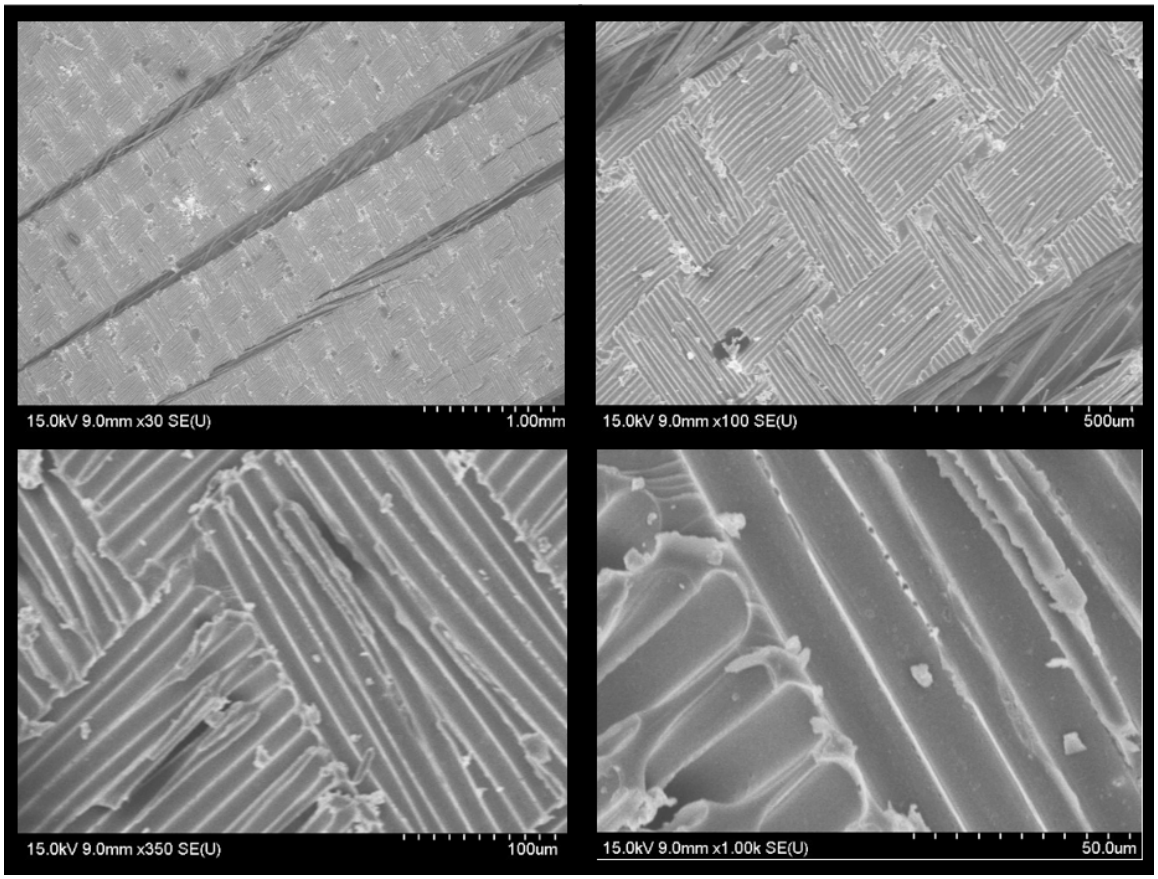

Figure 35: SEM images of the HiMassSEE Ground Control coupon – GC-1-1

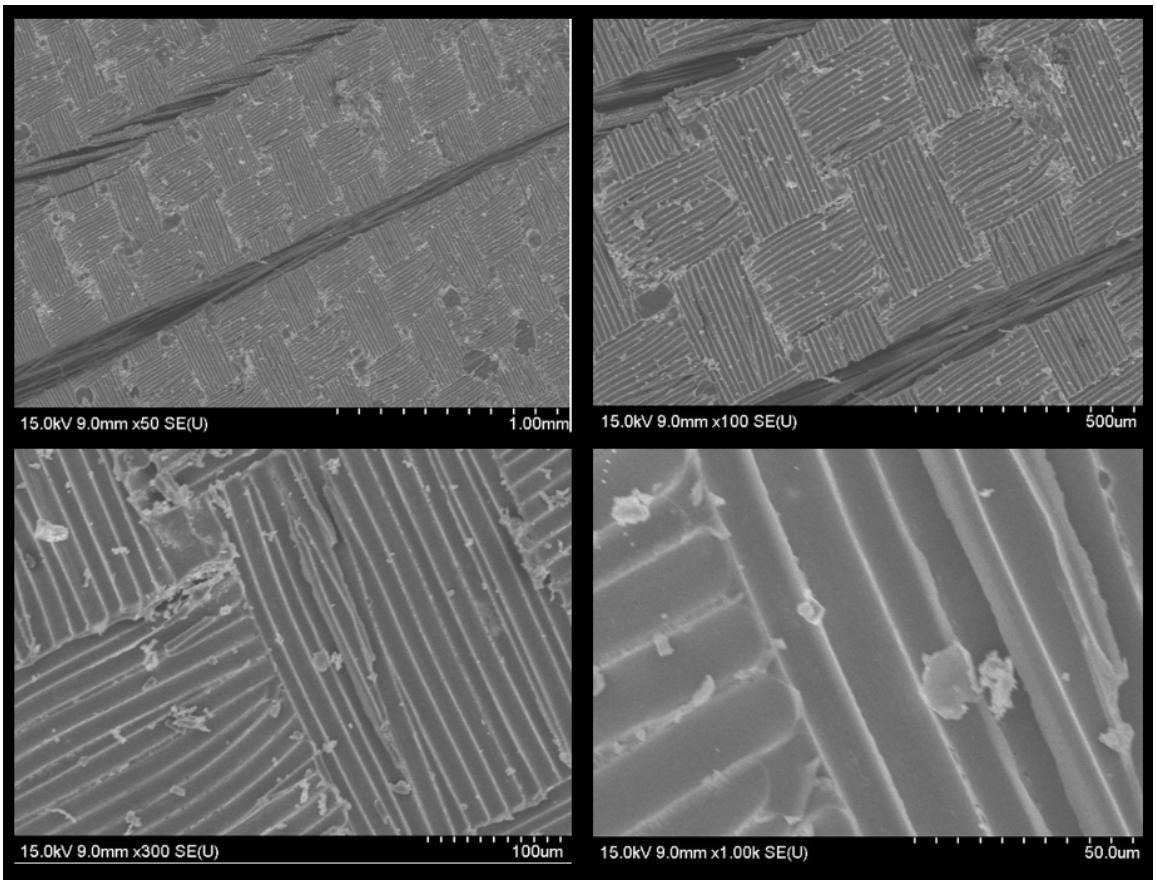

Figure 36: SEM Imagines of the HiMassSEE Flight Controls (No-Foil) coupon– CFCDET-1

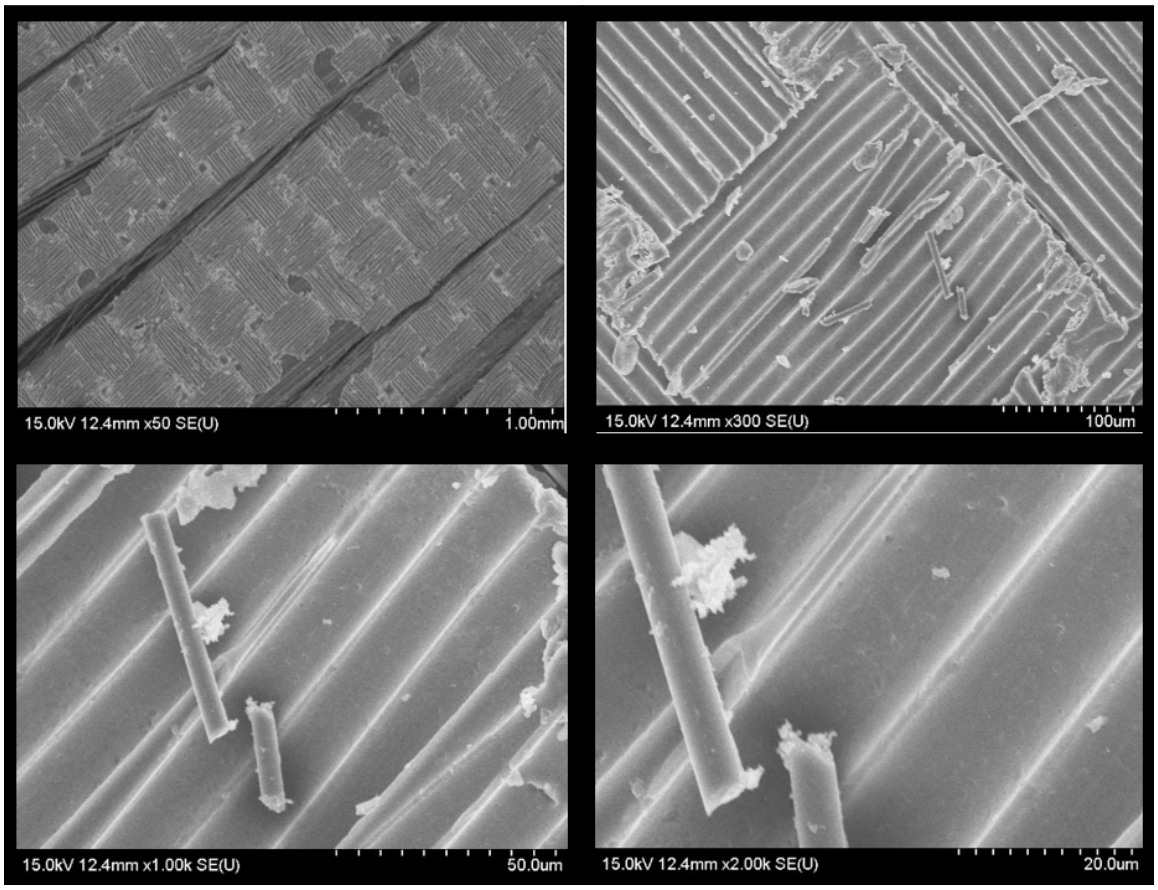

Figure 37: SEM Imagines of the HiMassSEE Niobium (Nb) coupons – CFCDET-2

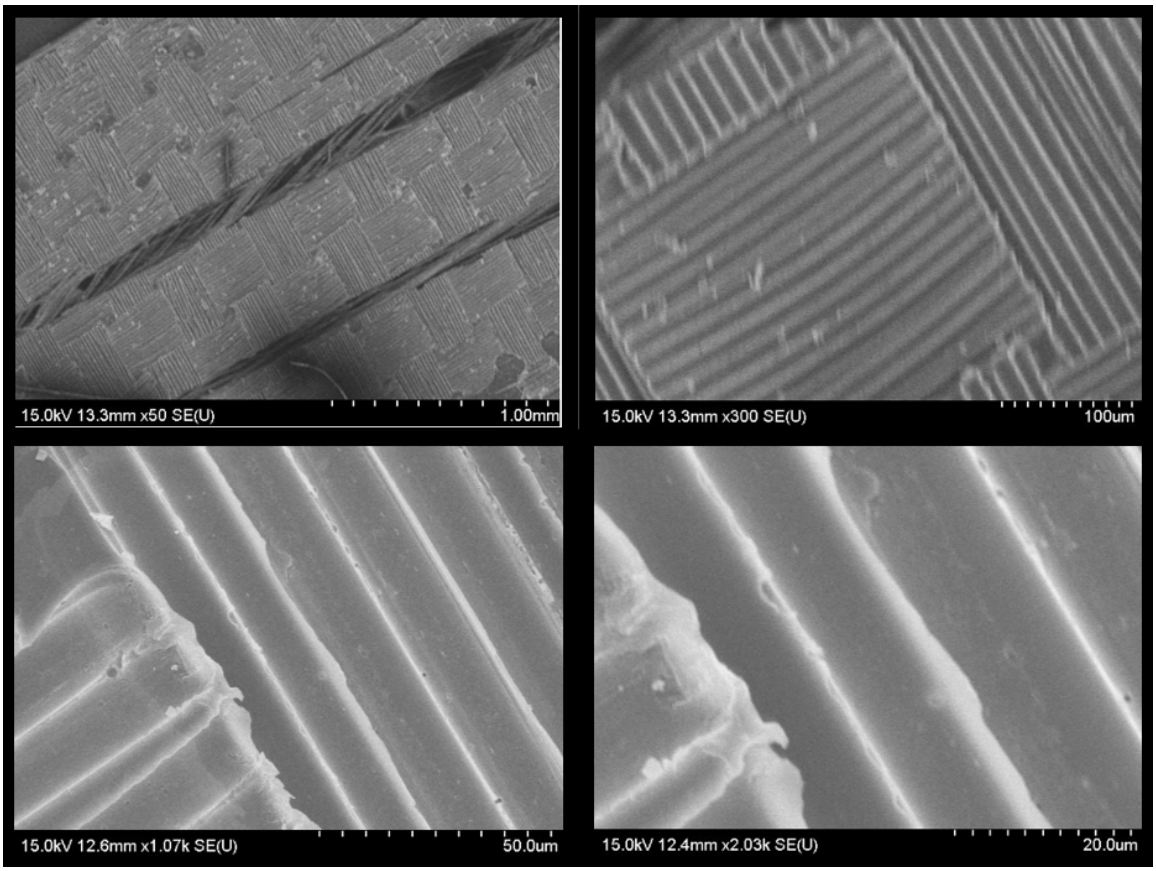

Figure 38: SEM Imagines of the HiMassSEE Tungsten (W) coupons – CFCDET-3

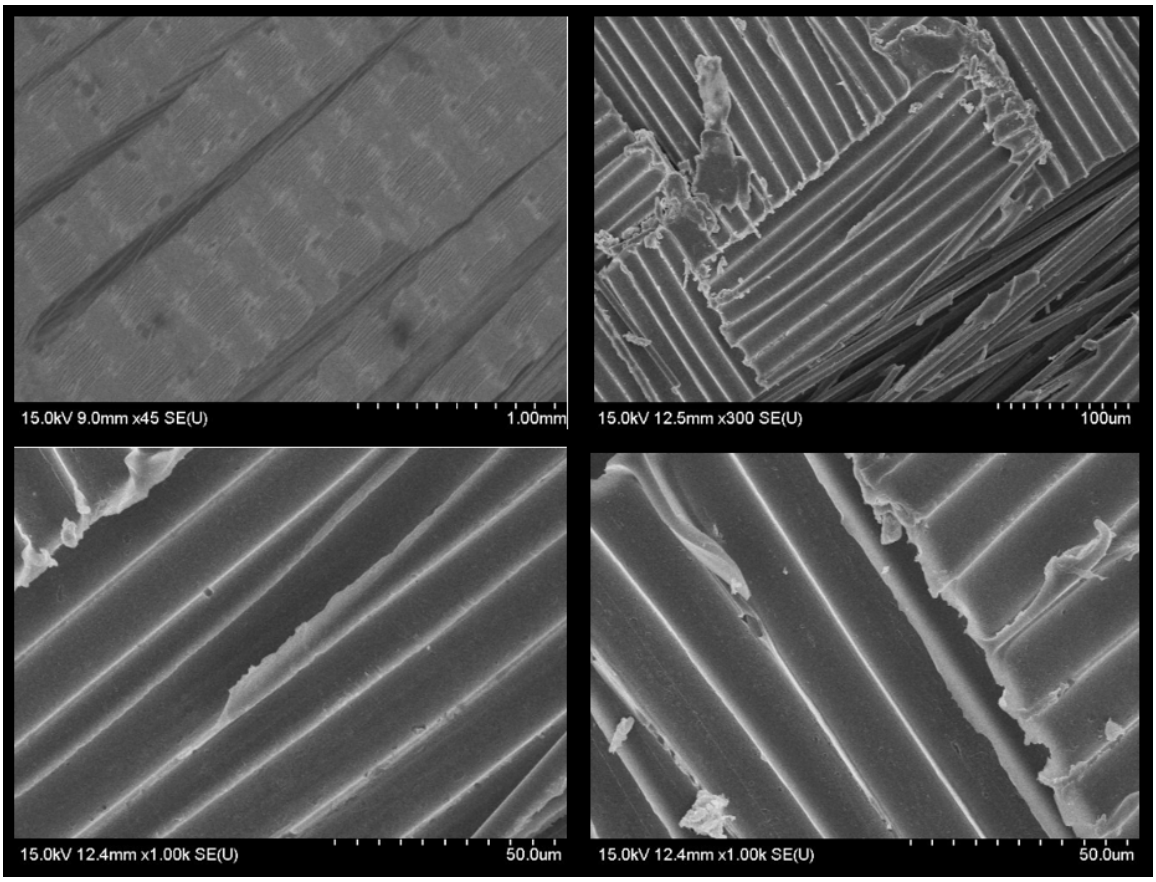

Figure 39: SEM Imagines of the HiMassSEE Lead (Pb) coupons – CFCDET-4

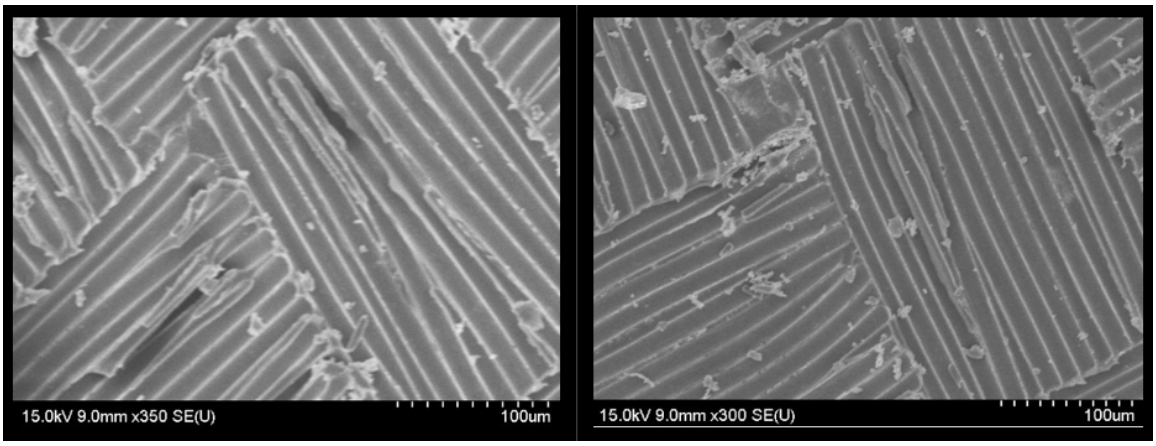

Figure 40: SEM Imagines of the HiMassSEE Ground Control GC- 1 vs. Flight control (No-Foil) CFCDET-4 Coupons

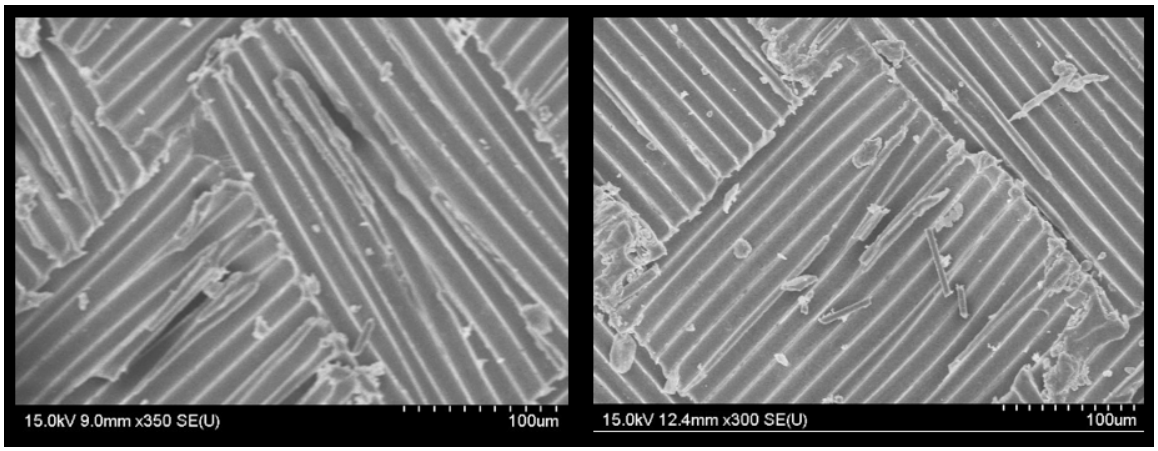

Figure 41: SEM Imagines of the HiMassSEE Ground Control GC- 1 vs. Niobium (Nb) CFCDET-2 Coupons

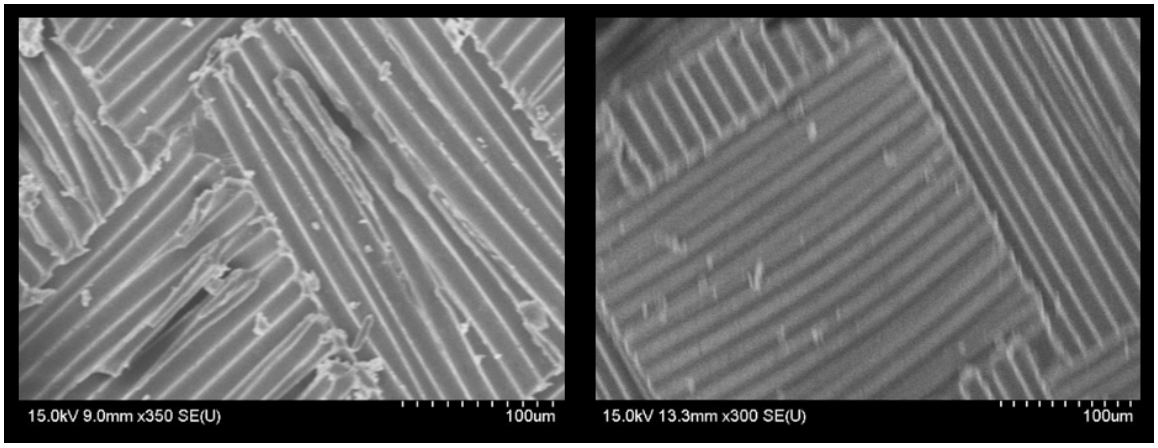

Figure 42: SEM Imagines of the HiMassSEE Ground Control GC- 1 vs. Tungsten (W) CFCDET-3 Coupons

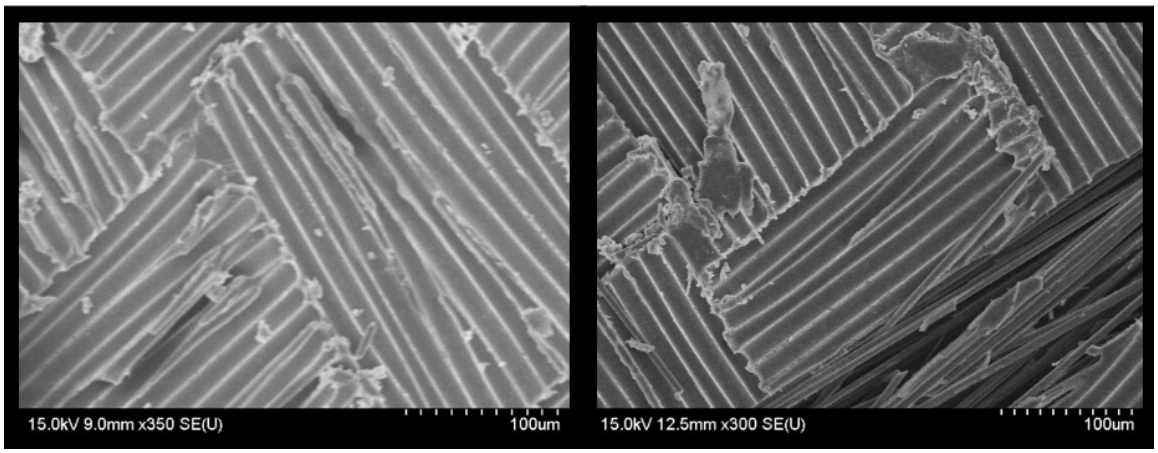

Figure 43: SEM Imagines of the HiMassSEE Ground Control GC- 1 vs. Lead (Pb) CFCDET-4 Coupons

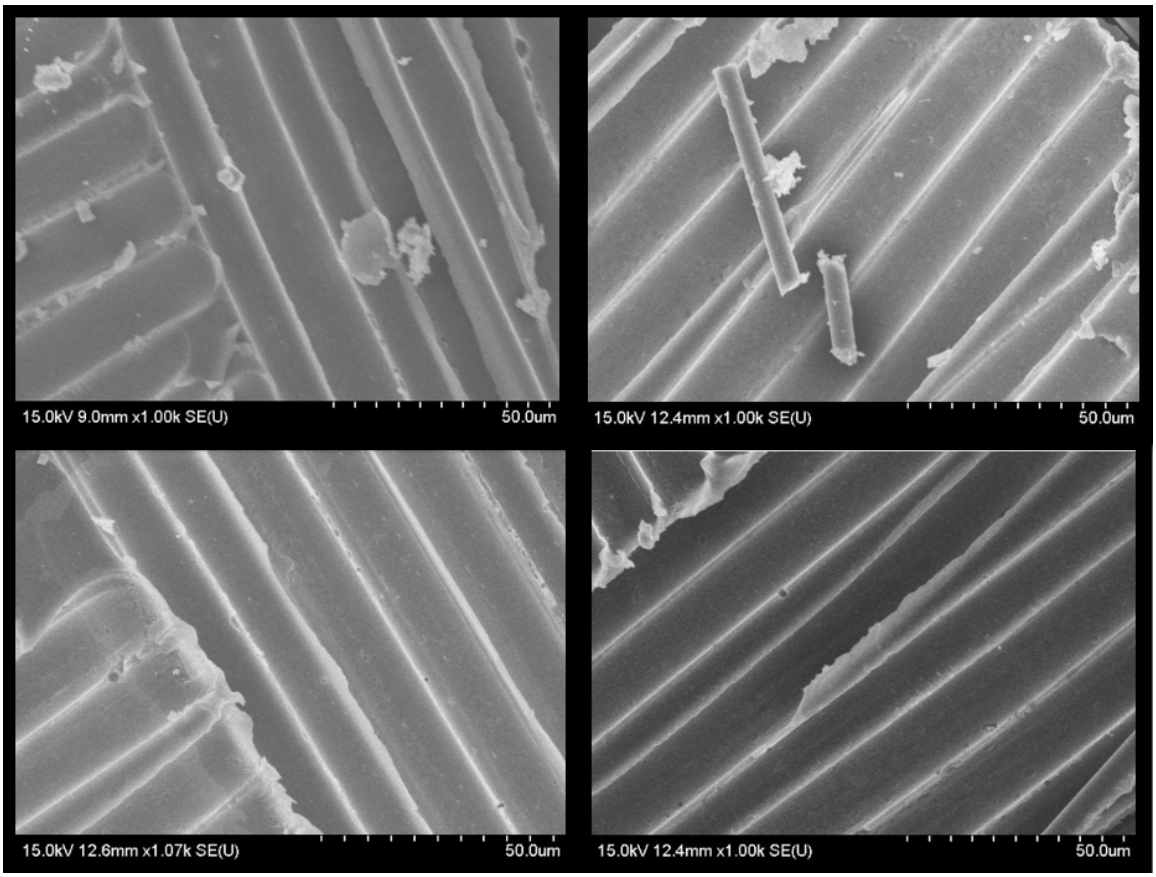

Figure 44: SEM Imagines of the HiMassSEE Flight Control CFCDET-1 (Top left), Niobium CFCDET-2 (Top right), Tungsten CFCDET-3 (Bottom left) and Lead CFCDET-4 coupon compared to each other.

3.1.4.2 MISSE-11 Results

SEM images of the MISSE-11 coupons was performed to determine the if the exposure to radiation and its effects on the surface of the carbon fiber coupons was greater than what was seen on the HiMassSEE coupons which were inside the pressurized volume of the ISS. Like the HiMassSEE coupons from section 3.1.4.1 above, the areas of interest are whether there are signs of impacts on the surface of the composite. The other area of interest was whether there was a noticeable difference in the degradation of the matrix through observed exposed fibers that appears to not be adhered in the epoxy. In Figure 45 below, SEM images were taken of the non-irradiated CFRP coupons from MISSE-11. The various images indicate strong adhesion between the carbon fibers and the matrix. Figure

46 are SEM images of the exposed irradiated CFRP coupons which were external to the pressurized volume on ISS. It was unknown which side was facing outer space and which side was facing towards earth. However, based on the images, there appears to be a noticeable amount of radiation impacts into the epoxy matrix, which are seen by the white marks on the surface of the composite. There is however no change that is discernible in the interface between the carbon fibers and the matrix Thus, the CF material did not experience an effect in the interface between the fiber and the matrix because of radiation exposure. There were no cross sections of the coupons taken in which a depth of the impacts could be determined, however through visual observation there appears to be no broken fibers which would indicate anything of a great speed hitting the surface of the coupon. Like the HiMassSEE coupons, there is likewise no ability to decern track marks created by radiation such as protons impacts. Figure 47 is a comparative set of SEM images of the exposed verses non exposed coupons.

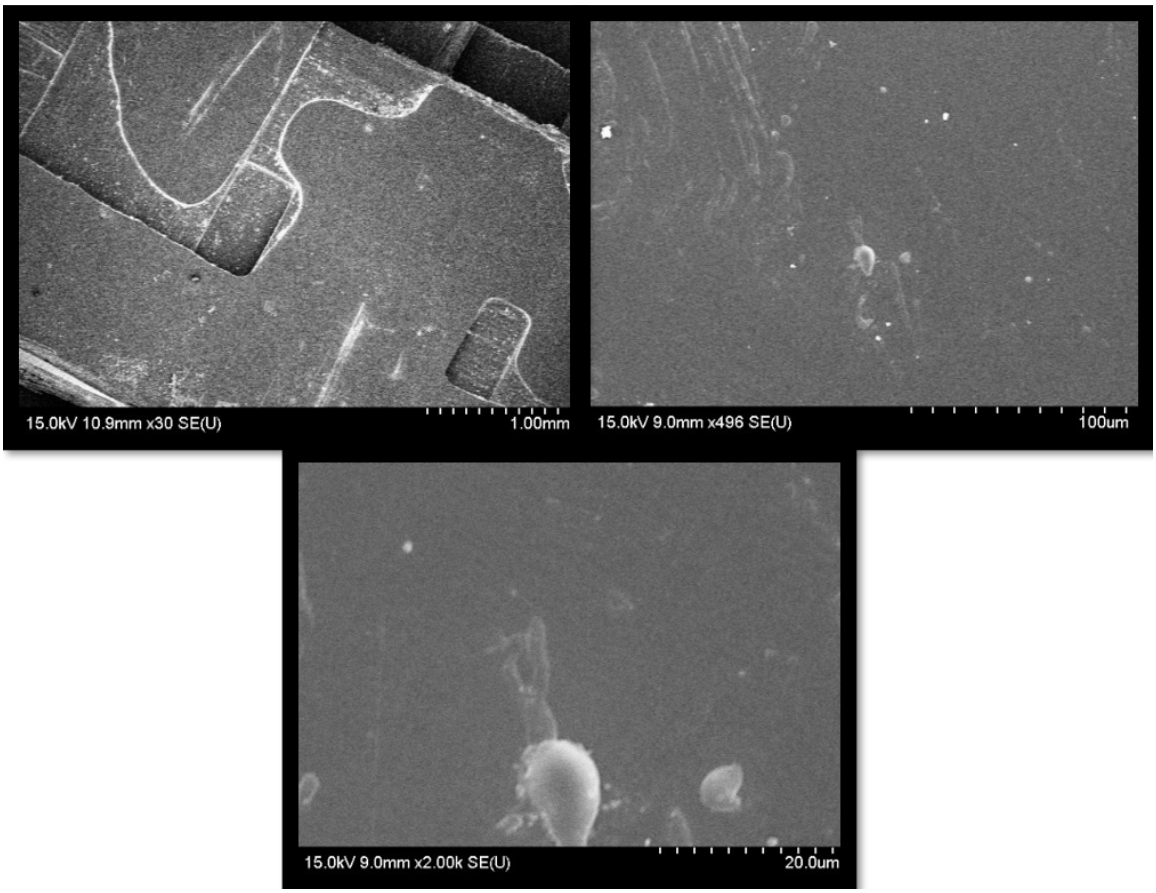

Figure 45: MISSE-11 Non-Irradiated Coupons – CFRP(u) - 1 - 1 and CFRP(u) - 1 - 2

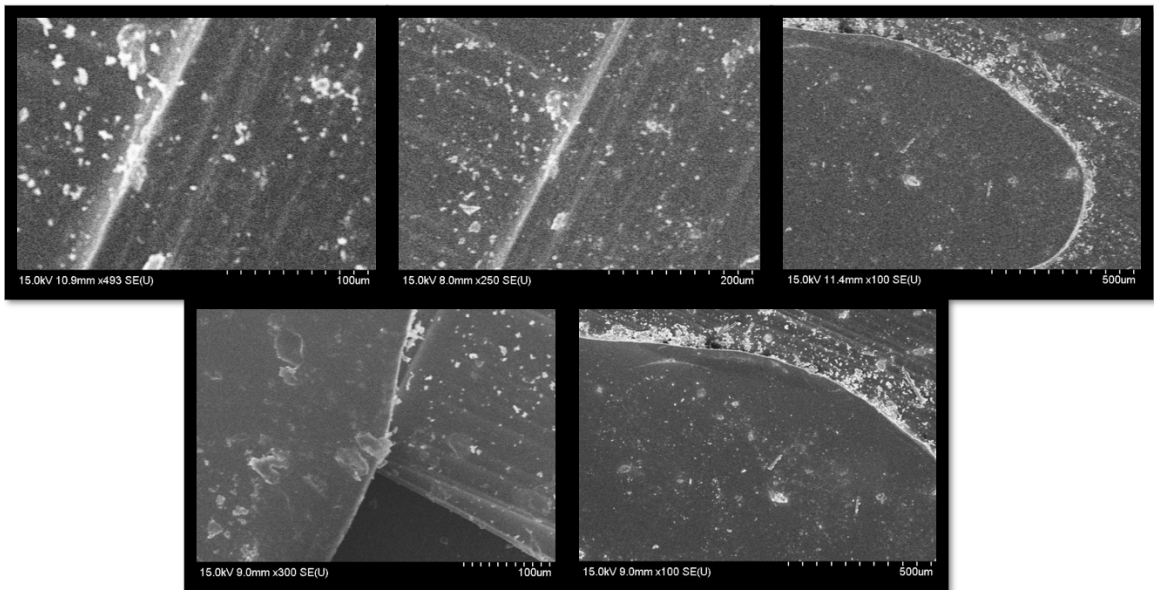

Figure 46: MISSE-11 Irradiated Coupons – CFRP (e) - 1 – 1 and CFRP (e) - 1 - 2

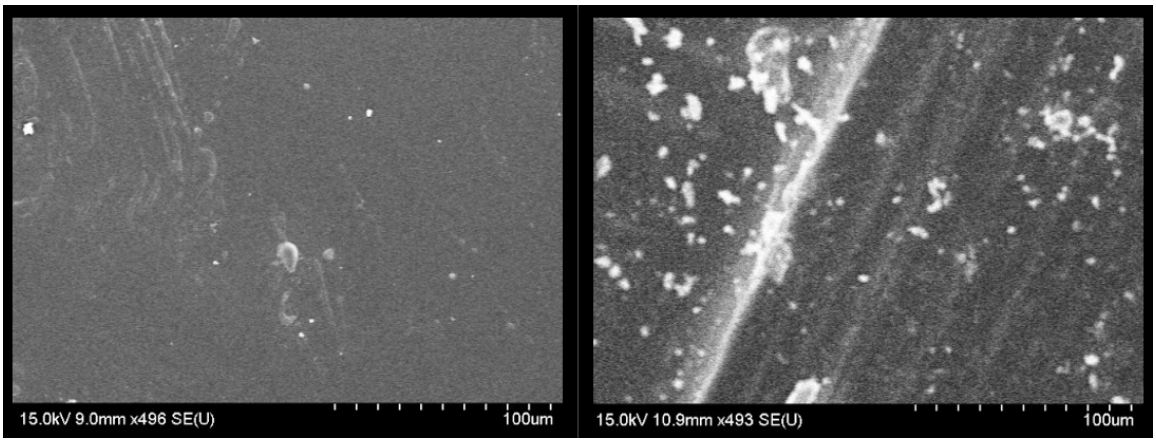

Figure 47: Comparison of MISSE-11 Coupons Non-Irradiated (Left) and Irradiated (Right)

3.2 Radiation Exposure

3.2.1 HiMassSEE Coupon Exposure

The International Space Station (ISS) operates at altitudes near 400 km with an orbital inclination of 51.6º. ISS orbits at a wide range of latitudes, longitudes, and space radiation environments. In these environments, radiation causes nuclear and radiation chemistry effects internal and external to ISS. It has been studied that at higher latitude, ISS is exposed primarily to very high kinetic (GCRs) and that approximately 80% of electronic and avionic anomalies are due to single event errors (SEE) occurring in these regions. At lower latitudes there is a reduced amount of SEE due to geomagnetic shielding and approximately 20% of the total SEE count occurs at low latitude, where the ISS is exposed to a high flux of lower energy charged particles. Because of these changes and the shielding mass remaining the same no matter what latitude ISS is in; SEEs occur at different rates. This can be attributed to the reasoning that as SEE rates increase at higher latitudes and shield mass and type remains constant (meaning unchanged), secondary particle showers occur due to spallation. Figure 48 and Figure 49, display graphically the

differences of SEE of Multiplexer/Demultiplexer (MDM) internal and external to ISS in the different regions. [3, 4]

Knowledge gained from experiments with CR-39 (Figure 4) demonstrated that while composites are different materials than CR-39 and other materials that are used in electronic and avionics, there is still the possibilities that these secondary impacts can be occurring in the matrix material due to materials around the composites. The composites coupons that were flown on ISS, did not have thermoluminescence detectors (TLDs) inside the carrying case and there was no way to measure the exact dose that the coupons saw when in orbit. However, based on review of In-flight TLD measurements inside ISS during solar max ranged from 4.5 cGy to 8.2 cGy per year. Pre-flight annual dose estimates for the US Lab module range from 8 cGy to 21 cGy with an average of 14 cGy due to location and region of ISS. This was well below the annual worst-case Design/Verification Environment (SSP-30512) doses at the corresponding shielding thicknesses (10^6 cGy at 0.0 g/cm^2, and 3 x 10^5 cGy at 0.9g/cm^2). [3, 4]

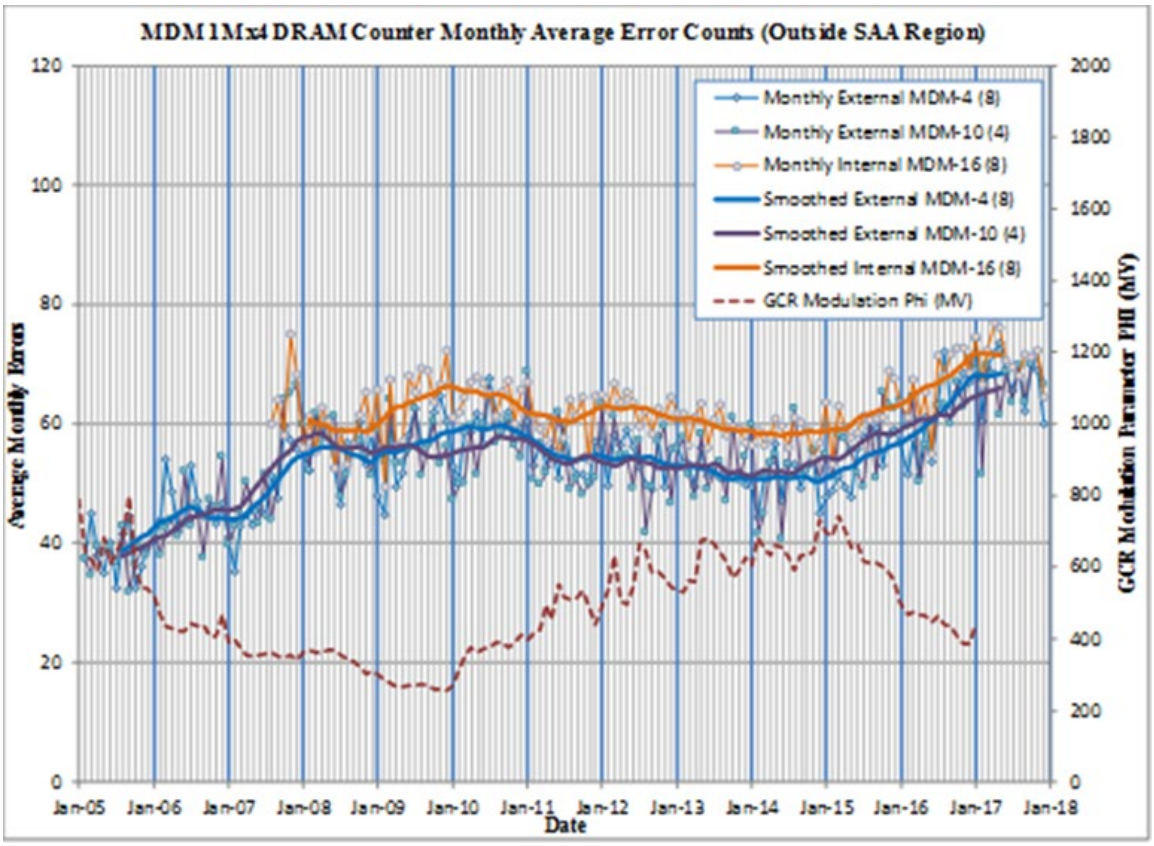

Figure 48: GCR region (higher latitude) MDM DRAM SEU monthly rates for internal and external MDMs between 2005 and 2018

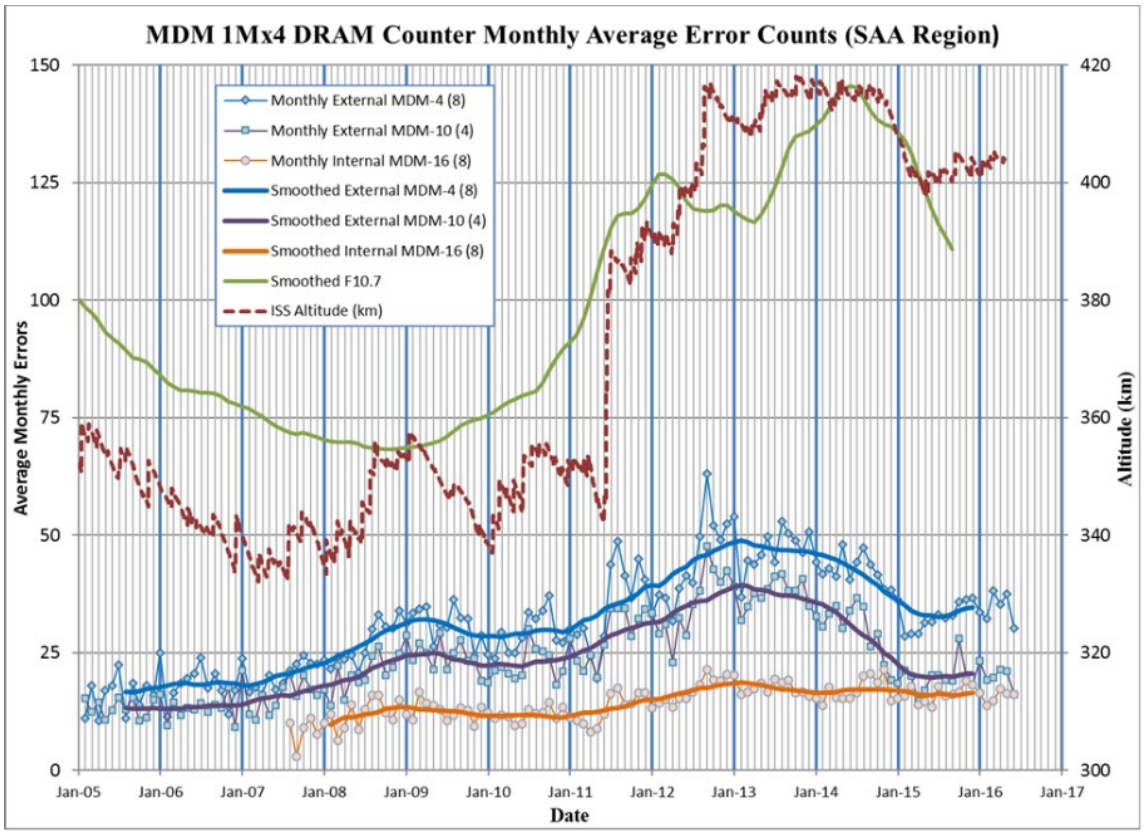

Figure 49: Lower latitude MDM DRAM SEU monthly rates for internal and external MDMs between 2005 and 2018

3.2.2 MISSE-11 Coupon Exposure

Prior work from Dr. Eric Benton's lab at Oklahoma State University was modelled and provided below to estimate the exposure rates at which the MISSE-11 samples saw while in orbit. Figure 50 below is the normalized daily dose for polyethylene versus the shielding depth in semi-log scale. The left end of the OLTARIS curve shoots up exponentially since most of the low energy protons from the trapped belt is stopped by the outer layer of the sample. As a result, most of the energy is deposited into the shallower depth part of the material.

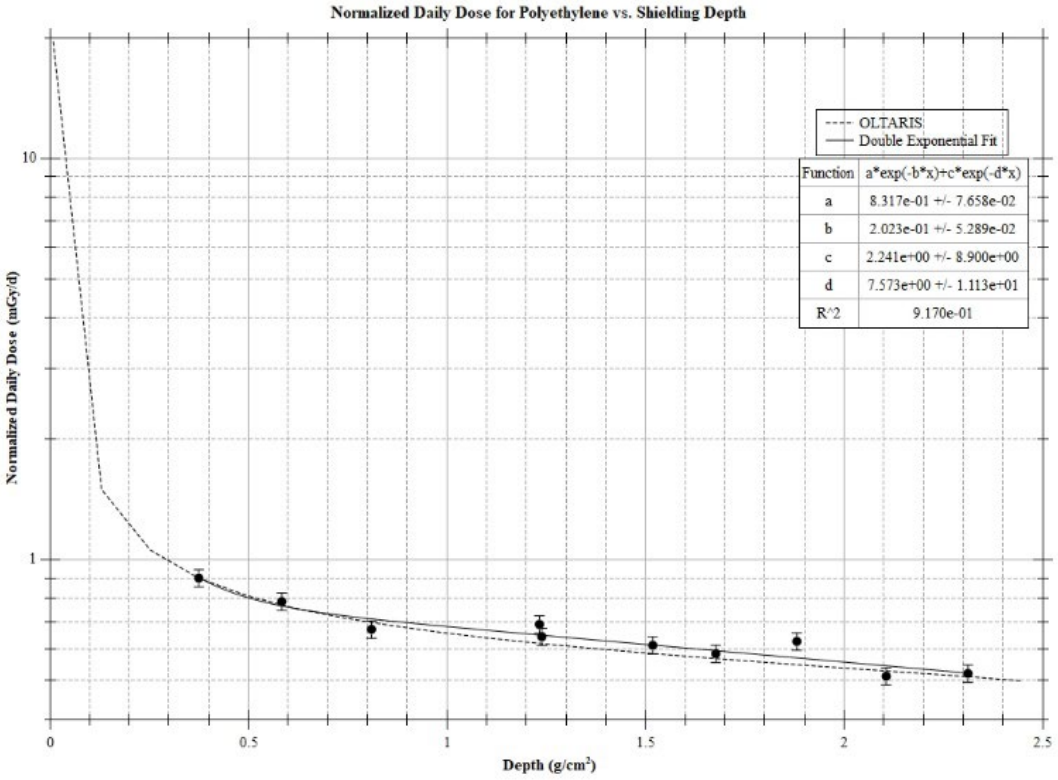

Figure 50: Normalized daily dose for polyethylene versus the shielding depth in semi-log scale

Figure 51 below shows models that were run to depict the normalized daily dose for aluminum versus the shielding depth in semi-log scale. Once again, the left end of the OLTARIS curve shoots up exponentially since most of the low energy protons from the trapped belt is stopped by the outer layer of the sample. As a result, most of the energy is deposited into the shallower depth part of the material.

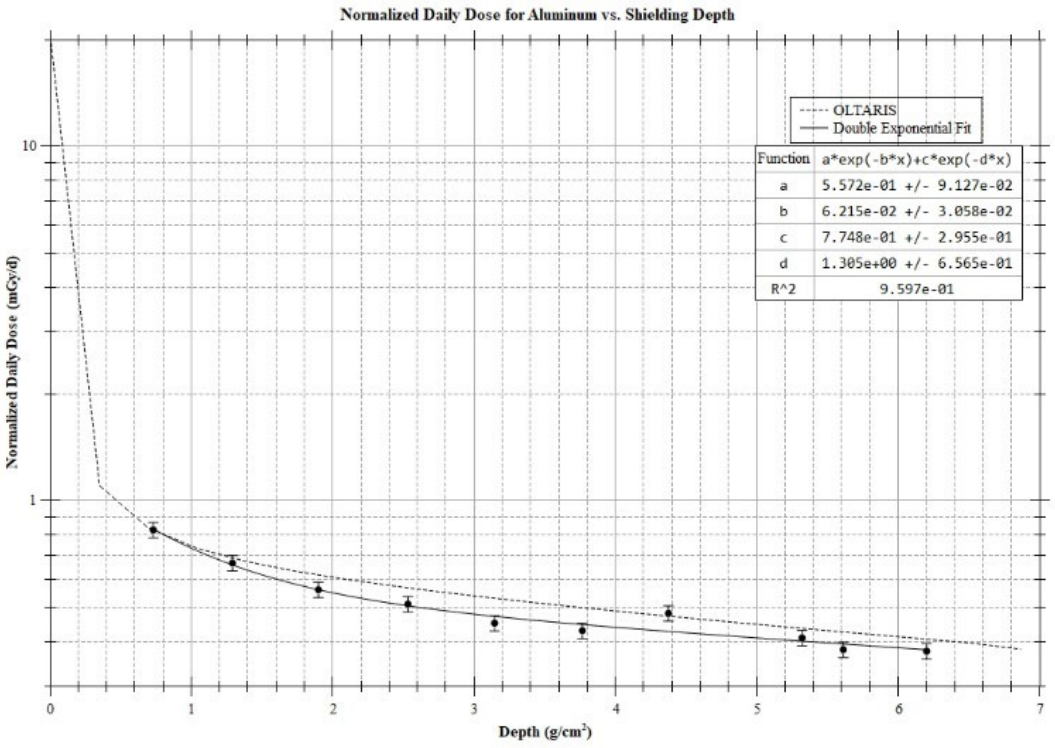

Figure 51: Normalized daily dose for aluminum versus the shielding depth in semi-log scale

Figure 52 below demonstrates the normalized daily dose for SC2020 versus the shielding depth on a linear scale. The drastic exponential decay is not observed in this plot since SC2020 was covered by rather thick carbon composite face plates, which stopped all low energy protons from entering SC2020.

In each of the above model runs, there is a common characteristic in all of them, which is that the impact depth is shallow. For the aluminum face sheets there is similarity to the curves from the polyethylene, however the composite face sheets appeared to provide better radiation absorption, which was able to stop a considerable amount of the low energy protons.

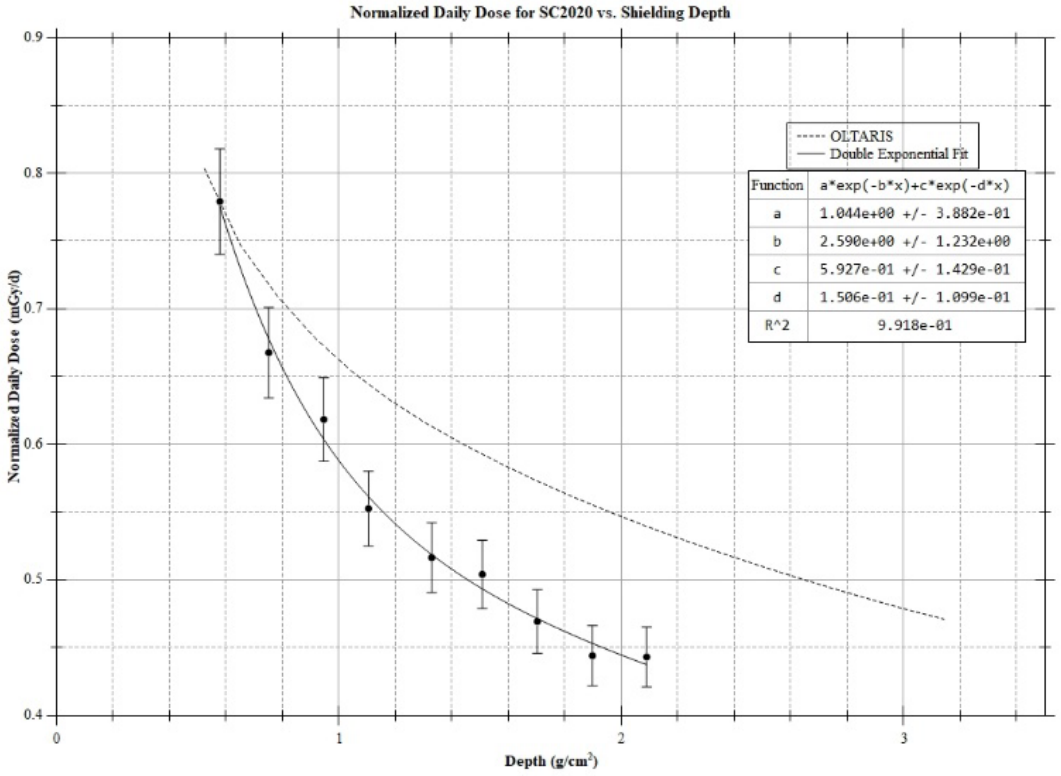

Figure 52: Normalized daily dose for SC2020 versus the shielding depth in linear scale

CHAPTER IV

DISCUSSION

4.1 Characterization Tests

4.1.1 Mechanical Testing

Due to the size constraints of the HiMassSEE carbon coupons and the MISSE-11 carbon coupons, it was not possible to perform tensile testing in the material labs at both Oklahoma State University and JSC Material labs. The alternative was to perform them using a micro load frame developed at White Sand Test Facility. However, factors such as the specimen width, the gauge length of the specimens, and the strands being joined to each other during the manufacturing limited the width of the samples from being fitted into the instrument for testing. The MISSE-11 coupons were too large for the micro-load frame. Another concern that came up when examining the HiMassSEE coupons was that for tabbing the coupons, they would need to be separated into individual tows. While separating the coupons into tows, the tows were damaged, and the testing could have presented inaccurate results due to the damage occurring while trying to separate the tows. While this data would have provided mechanical properties of the composites, it is very likely that it would not have provided any new information related to composite degradation. Prior testing had shown that mechanical properties of composites were not greatly affected after being irradiated due to the radiation not affecting the carbon fibers themselves. Composite structures and pressurized tanks are fiber dominated systems and due to the radiation having no effect on the fibers themselves there is little change that has been found in prior studies.

Dynamic mechanical analysis (DMA) was selected as a testing method in which data could be collected on the MISSE-11 carbon coupons. Unfortunately, the HiMassSEE coupons dimensions were not large enough to perform DMA tests on. Storage modulus, loss of modulus and the damping factor (Tan Delta) were all collected and compared to each other. There were no significant changes between the ground and flight coupons, however on coupon CFRP (e)-1-2 (irradiated outside of ISS) there was a noticeable change is storage modulus and loss of modulus from both the ground controls and CFRP (e)-1-1 (irradiated outside of ISS). All MISSE-11 coupons were prepared using the same maunfacuting process controls and using same batch of starting materials. The testing methods were identical for all coupons when peforming the DMA testing. The differences between the ground control and the flight controls can be related to the environmental changes and the exposure to radiation which would create molecular changes within the materials that would lead to cross-linking and chain scission. There could also be a change is the material softening which would point to the reason of storage modulus reduction and loss of modulus.

The CFRP(e)-1-1 and CFRP(e)-1-2 samples, while both were irradiated during the same period and same location outside of ISS, have some differences. The difference between CFRP (e)-1-1 and CFRP (e)-1-2 in storage modulus is 2889MPA or 5.6% reduction. In order to examine the difference between the ground controls and the flight controls, the results of the ground controls were combined and averaged and then compared to each individual flight coupons. For CFRP (e)-1-1 there was a 2.8% increase in storage modulus versus the ground control. Matrix stiffness due to irradiation is atttributing to the increase in storage modulus. For CFRP (e)-1-2 however the storage modulus decreased

verses the mean value of the ground control coupons. The difference was 2.9% reduction in storage modulus. The only explanation for the reduction is that each side of the test frame could have experienced a different dose of the radiation and type of radiation. The assumption, due to the lack knowledge of coupon orinentation being outside the zenth direction of on ISS, is that CFRP (e)-1-2 could have faced a direction that was exposed to a larger dose of atomic oxygen. This assumption is based on the visual inspection of the coupon when it was returned to the ground. These coupons displayed a discoloration on the outer surface which can be contributed to atomic radiation from the earth atmosphere.

Like the storage modulus, the loss modulus likewise showed an increase in loss modulus on CFRP (e)-1-1. The increase of the mean value of the ground control results was 4.5% . Similar to the storage modulus, the increase was likely due to the exposure of radiation due to which the matrix could have stiffened. For CFRP (e)-1-2 however the decrease in loss modulus was much greater than what was seen on the storage modulus. The decrease compared to the mean value of the ground control coupons was 15.5% decrease. A decrease of 15.5% has a significant impact to the ability of the composites to retain its stiffness/hardness. The difference between CFRP (e)-1-1 and CFRP (e)-1-2 likewise was larger than the difference in the storage modulus, which was 20%. The direction and orientation of the coupon while in orbit was likely the source of the difference between CFRP (e)-1-1 and CFRP (e)-1-2. The glass transition temperatures for each of the MISSE-11 coupons were all within five degrees celcius of each other. There was a slight reduction in the glass transition temperature for the exposed MISSE samples compared to the ground controls, which suggests that the radiation exposure and cross-linking could have contributed to this reduction and softening. The general rule with polymers is that a

decrease in glass transition indicates that degradation of the material properties that has occurred.

4.1.2 Differential Scanning Calorimetry (DSC)

DSC was selected in order to determine if additional cross-linking or chain scission was occuring in the HiMassSEE coupons that were flown inside the internal pressurized volume on ISS. The assumption was that as the coupons were irradiated while in orbit, there would be a change in the molecular structure of the coupons which would be shown through cross-linking or chain scission. Due to each of the coupons having a different metallic foil between them it was also assumed that the larger atomic number foils would produce a secondary particle shower on the coupons which would then effect the results of the DSC to demostrate that the matrix material was indeed going through a molecular transformation.

When the data was plotted however there did not appear to be any significant changes in the material. There were no cure peaks that occurred in the coupons in the first heat cycle, which could demonstrate that all the coupons were full cross-linked prior to being irradiated. There was no major difference between the ground controls and the flight coupons. When the coupons were compared to each other, there was no noticeable curing peaks found. The data was collected at an initial rate of 5°C/min; however, the rate of data collection could have been so fast that it could not record all the peaks. There were limited flight coupons to test on and when a second test was run at 3°C/min, it was noticed that there were slightly more defined peaks compared to 5°C/min . However, the second tests were run after the flight coupons had already been tested. The only difference that was

observed in the original data was that the slope in data from the ground control coupons was not as sharp as the flight controls. This change in slope could be a sign that the coupons could have undergone surface level chain scission and oxidation. The factors that could enhance the scission effects are the chemical composition of the epoxy through the presence of toughening agents. While the chemical composition of the epoxy matrix was not disclosed due to being proprietary, it is a known fact that the epoxy has toughening agents mixed into the epoxy for improving damage tolerance. There has been research completed that suggests that toughening agents are more "susceptible to radiation damage and potentially enhance aging and expected increased radiation dose at the interface between the carbon fibers and the epoxy" [6, 7]. Research has also shown that chain scission has a higher probability to occur on a surface of a polymer that is exposed to oxygen. The samples were inside the pressurized volume inside of ISS, which means that they were exposed to a source of oxygen while being irradiated.

4.1.3 Fourier transform infrared Spectroscopy (FTIR)

FTIR was performed on the HiMassSEE coupons in order to deteremine the effects of the radiation on the coupons and for comparison to the non-irradiated coupons. The FTIR spectrum was examined and compared to prior research that suggested that typical epoxies that are common to aerospace are diglycidyl ether of bisphenol-A (DGEBA) [6 ,7] base. In comparison to this prior research, there are similarities between the epoxy used for the HiMassSEE samples and DGEBA, which confirms that toughing agents were present in the HiMassSEE coupons. As dicussed from the DSC section, the toughing agents are known to increase the probability of chain scission.

While it is known that the epoxy used on the HiMassSEE coupon are similar to that of DGEBA, it is also assumed that the epoxy also contains aromatic rings which would increase the resistance to radiation. The data shows that all HiMassSEE coupons had an increased aromaticity. Prior research suggested that the aromatic structure of the epoxies are less durable if the coupons are exposed to oxygen while being irradiated resulting in chain scission. Because of likelihood of chain scission in the epoxy, there is a icreased molecular mobility which increases radical recombination within the molecular structure of the epoxy. Since oxidation is not likely to cause enhanced degradation to the epoxy and only surface level damage, it is likely that chain scission is the dominating process of degradation of the epoxy for the HiMassSEE coupons.

When comparing the FTIR curves, there is an interesting aspect in all the peaks based on the metal foils that are separating the layers from each other. While there is an increase in the absorbance peak for the ground control and the flight control samples, they are similar. However when the coupons with tungsten and lead foils were plotted, the data showed a drastic uptick in the peaks, which suggested that as the atomic number of the material increases, there is increasing absorbance. Interesly the only HiMassSEE coupons with decreased absorbance below that of the ground control are the coupons that had niobium foils between them. The DSC results were also different for these samples from the others. It is unlikely that these samples were poorly processed and therefore, the only explanation is that the niobium foils could be providing some shielding from radiation. However this would have to be examined more closely before a conlcusion could be made.

4.1.4 Scanning Electron Microscope (SEM)

4.1.4.1 HiMasSEE Coupons

In the case of the HiMassSEE coupons, there was no visual marker that could be identified as track marks from secondary particle impacts. This is no surprise only for the reason that in past expirements that involved CR-39 and Mica PNTDs, the samples had to be etched with NaOH at 70 degrees centigrade for 6 hours while stirring constantly to see any track marks. By completing the chemical etching the pores would increase in size that could be observed using polarized light reflected microscopy. One advantage prior expirements had was that the samples were transparent and the track marks were able to be detected once etched. Prior to etching however not even the use of a SEM could pick up the track marks from particle impacts. For the carbon fiber composite coupons, there was no method of etching the material in a way to observe the tracks which are ultimately present, however unable to be seen without sizing the pores. During the chemical etching process, the epoxy would likely be damaged and no useful data could be recovered. No feasible methods of etching the composite coupons found based on literature survey.

The second portion of examination was to look for areas in which the epoxy was not fully encasing the fibers which would point to a degradation of the matrix. Through careful examination of the fibers at multiple resolutions and magnifications there were no indications that the epoxy was being degraded to the point of allowing the fibers to not be encased in the epoxy.

4.1.4.2 MISSE-11 Coupons

Similar to the HiMassSEE coupons, the MISSE-11 coupons were examined by SEM. Similar to the HiMassSEE coupons, the MISSE-11 coupons were examined for

particle impacts resulting in track marks in the surface of the coupons and whether the carbon fibers remained encased in the epoxy matrix. SEM images suggested that there was a difference between the ground controls and the flight coupons which were flown outside the pressurized volume of ISS. There was significant marks indicating impacts on the surface of the coupons that were exposed to radiation. While these evident markings were signs of impacts, no other tests were run to see what the depth of the impacts were due to needing the coupons for DMA testing and cross-sectioning would have resutled in lossing that ability due to the limited quanity of coupons.

It was also examined that the one of the coupons was slightly discolored on one side and the other coupon was not discolored on either side. The assumption in this case is that this coupon must have been exposed to atomic oxygen.

SEM images also did not suggest that the epoxy matrix was failing through degradation of the surface in which fibers were protruding throug the matrix. All fibers appeared to be securely encased in the expoy matrix.

4.2 Radiation Exposure

4.2.1 HiMassSEE Coupon Exposure

There was no experimental data collected for the radiation exposure doses for the HiMassSEE coupons, however based on heritage data and data collected inside the internal pressurized volume on ISS estimates were made. Through examination of the dose rates that are present inside of the pressurized volume of the ISS, there is a considerable amount of margin seen between these dose rates and experimental data from heavy element accelerators on earth. According to collected data, composites with an epoxy matrix was

needed to receive a threshold damage dose of 10^8 cGy [4] in order for damage to begin to affect the mechanical properties and performance of the composite. This is shown through the characterization that was completed on these coupons. While there was a noticeable change in the molecular structure of the coupons, there was not damage which produced a failure mode in which would not be covered by the safety margin in a system design.

4.2.2 MISSE-11 Coupon Exposure

Through examination of models provided by Dr. Eric Benton's lab, the composite face sheets provided an excellent shielding for low energy protons from entering the SC2020 coupons. Modeling dose rates can be a difficult process due to the environment being highly variable due to the altitude, latitude, solar activity and solar cycle effects. When in the lower latitude region ISS is primarily shield from GRC. However at both low and high latitudes ISS sees both trapped radiation (protons and electrons) and GRC. Results from the TLD measurements on the MISSE-11 SC2020 coupons revealed that at the shielding depth of 0.5 g/cm^2, a 26 cGy dose rate was recorded. At this rate the level of radiation dosing is well below the 10^8 cGy threshold for damaging composite structures. The data collected from the DMA testing demonstrated that even though the carbon face sheets adsorbed a lot of the estimated radiation, the mechanical properties were not significantly affected, except on CFRP (e)-1-2 coupons which it is assumed to have been exposed to high doses of the atomic oxygen due to the discoloration of the one of the sides of the coupon.

CHAPTER V

CONCLUSIONS

The study that was completed on the HiMassSEE coupons and the MISSE-11 coupons was focused on radiation dose rates that were observed inside the pressurized volume and the external environment of ISS. These dose rates were far below those that have been previously studied which typically were performed using high energy particle accelerators and were able to produce dose rates above 10^8 cGy before significant changes were observed in the material properties. However, these studies are expected to be more representative of the actual space radiation levels that could be observed during actual space flights. Though the data that was collected throughout the experiments was small and only minimal or subtle changes were observed in the mechanical properties, which suggested that the samples were experiencing a small but noticeable molecular change. There was evidence of mild chain scission and oxidation that formed on the surface levels of the coupon however not to the level of which is appeared to disrupt the adhesion of the fibers inside the matrix. This resulted in very minor changes in the glass transition temperature in the exposed samples.

Interestingly there was a notable increase in the absorbance peaks on the FTIR results that showed that the HiMassSEE coupons did in fact have some molecular changes based on the atomic number of the metallic foils introduced between the composite samples. There was also an observation that Niobium might be a potential source of

shielding. However, this data needs to be further investigated prior to any conclusions that can be made.

The main conclusion that can be drawn from the experiments and resulting data is that the margins that are built into the designs of spacecrafts and hardware component (outside of avionics and electronic) are sufficient in protecting against a degradation of the composite material to the degree of failure in LEO. This information is highly valued for future missions in which commercial elements are going to form new programs such as Commercial Low Earth Orbit (CommLEO). However, there is still the concern to further understand the environments in which spacecraft and habitats will encounter outside of LEO where little studies have been completed. “The lifetime and safety ratings of these materials could be impacted as a result of this information and therefore is critical for use of these composites in the deep-space environment.” [6,7]

CHAPTER VI

SUGGESTED FUTURE WORK

There are multiple areas which still need to be studied in the field of composites that are operating in environments of space radiation outside of LEO. One of these areas is that in general heritage missions to the LEO and the lunar surface have been based on "take what you need to complete the mission and return home on empty" regarding environmental life support services (ECLSS) and propellants. However, as NASA's missions continue to evolve further from LEO, the idea of providing refueling options are becoming a reality. Unfortunately, this reality also brings about concerns regarding the radiation effect on composites that are now being dynamically cycled in the presence of radiation doses that have not been fully studied or understood outside of prediction models. It is understood from prior studies, including the ones completed here that there are effects such as cross-linking, chain scission, oxidation degradation and minute changes in glass transition temperature that occurs in composites even in low dose environments. The margins have always been conservative due to the reason that the composites have loads (energy) that are decreasing in time. However, with the knowledge that these same composites are now going to be required to experience this degradation for longer periods of time and have continued dynamic loads placed on them this is an increase in risk that is not fully understood and required investigation to know how to bound the risk to future missions.

The experiments performed in the past have provided confidence in the structural capabilities of composites, however that does not mean that these experiments are relatable to fully understand risk of future mission. For future work, there needs to be examination of the composites outside of the typical testing of material strengths. We understand through heritage testing that strength of composites is not all that effected due to the fibers being the dominant material in the composite. We need to understand more closely what the matrix is doing in dynamic cyclic loading while being introduced to radiation, i.e, under synergistic conditions. There have been initial tests that have been performed to examine these questions, however the results presented negligible results due to the gripping method and the sample sizes used. Investment into studies that does not limit the sample sizes so that the gripping methods were not going to affect the test results could potentially bring confidence and risk reduction into these unanswered questions.

From the experiments completed in this research, an area of study that needs to be reexamined are the results found with the HiMassSEE niobium foil coupons. The results showed that these were unique in the characterization results, and it needs to be understood if this uniqueness is due to an anomaly or a new discovery.

REFERENCES

[1] NASA, "July 20, 1969: One Giant Leap for Mankind," NASA, 20 July 2019. [Online]. Available: https://www.nasa.gov/mission_pages/pollo/apollo11.html.

[2] K. Herrman, “Mechanical and radiation shielding properties of boron nitride reinforced high-density polyethylene”, Oklahoma State University, July 2020

[3] S. L. Koontz “The Nuclear Chemistry and Physics of Galactic Cosmic Ray and Van Allen Belt Charged Particle Interactions with the International Space Station” .[Unpublished], NASA Johnson Space Center 2019

[4] S. L. Koontz “Space Flight Ionizing Radiation Environments” [Presentation]. NASA Johnson Space Center June 29, 2019

[5] M. Al-Sheikhly, A. Christou, “Tutorial How Radiation Affect Polymeric Materials”. IEEE Transactions on Reliability, vol. 43, no. 4, December 1994

[6] K. Rojdev “Long Term Lunar Radiation Degradation Of Potential Lunar Habitat Composite Materials”. [Dissertation]. Faculty Of The USC Graduate School University Of Southern California, December 2012

[7] K Rojdev, MJ. E. O’Rourke, C. Hill, S. Nutt, W. Atwell, “Radiation effects on composites for long-duration lunar habitats”. Journal of Composite Materials 2014, Vol. 48(7) 861–878. 2013

[8] R.D. Gilbert, R. E. Fornes, J. D. Memory “Effects of High Energy Radiation on Mechanical Properties of Epoxy Graphite Fiber Reinforced Composites”. NASA Grant 1562- S6, January 1983 – December 1983

[9] A. Denaro. “Fundamentals of Radiation Chemistry”. Ann Arbor Science Publishers, Inc., 1972.

[10] M. Nevarez, J. M. Waller, Regor L. Saulsberry. “Characterization of Space Radiation Effects on Composite Overwrapped Pressure Vessels for the International Space Station”. [Unpublished], NASA Johnson Space Center – White Sands Test Facility, July 2013

[11] W. Parkinson and O. Sisman. “The Use of Plastics and Elastomers in Nuclear Radiation”. Nuclear Engineering and Design, 17: 247-280, 1971

[12] J. Spinks, and R. Woods. “An Introduction to Radiation Chemistry”. John Wiley & Sons, Inc., 3rd edition, 1990.

[13] J. O’Donnell and D. Sangster. “Principle of Radiation Chemistry”. American Elsevier Publishing Company, Inc., 1970

[14] D. Clegg, and A. Collyer. “Irradiation Effects on Polymers”. Elsevier Science Publishers LTD, 1991

[15] E. Hoffman and T. Skidmore. “Radiation Effects on Epoxy/Carbon-Fiber Composite”. 2008. SRNL-STI-2008-00527

[16] E. Benton, R, Vaidyanathan. “Assessment of Radiation Shielding and Physical Properties of Novel and Baseline Materials through Exposure on the Outside of ISS”, [Unpublished] Oklahoma State University, 2020

[17] J. M. Waller, P. Spencer, R. L. Saulsberry. “Modal Acoustic Emission Coupled with Microscopy (mAE-SEM)”. [Unpublished], NASA Johnson Space Center – White Sands Test Facility, November 2008

[18] N. J. Greene, J. M. Waller, R. L . Saulsberry. “Technical Review of Empirical Based Creep Rupture Lifetime Prediction Methodologies Applicable to Composite Overwrapped Pressure Vessels and Related Composites Structures”. [Unpublished], NASA Johnson Space Center – White Sands Test Facility, November 2008

[19] J. Davenas, I. Stevenson, N. Celette, S. Cambon, J. Gardette, A. Rivaton, and L. Vignoud. “Stability of Polymers Under Ionizing Radiation: The Many Faces of Radiation Interactions with Polymers”. Nuclear Instruments and Methods in Physics Research, Section B, 191: 653-661, 2002.

[20] L. Vignoud, L. David, B. Sixou, and G. Vigier. “Influence of Electron Irradiation on the Mobility and on the Mechanical Properties of DGEBA / TETA Epoxy Resins”. Polymer, 42: 4657-4665, 2001.

[21] T. Sasuga and M. Hagiwara. “Disintegration of Network Structure of Bismaleimide-triazine Resin by Electron Beam Irradiation”. Polymer, 27: 681-685, 1986

[22] T. Murayama, and J. Bell. “Relation Between the Network Structure and Dynamic Mechanical Properties of a Typical Amine-Cured Epoxy Polymer”. Journal of Polymer Science, Part A-2, 8: 437-445, 1970

[23] L. Nielsen. “Cross-linking: Effect on Physical Properties of Polymers”. Journal of Macromolecular Science, Reviews in Macromolecular Chemistry and Physics, C3(1): 69-103, 1969.

[24] A. Kenyon, and L. Nielsen. “Characterization of Network Structure of Epoxy Resins by Dynamic Mechanical and Liquid Swelling Tests”. Journal of Macromolecular Science, Part A, 3(2): 275-295, 1969.

APPENDICES

Table A1: DSC Raw data for HiMassSEE Coupons

DSC raw data2.0.xlsx

Table A2: DMA Raw Data for MISSE-11 Coupons

DMA raw data.xlsx

Table A3: Raw Data for Radiation Exposure Model for MISSE-11 Coupons

Radiation Exposure Models Raw Data.xlsx

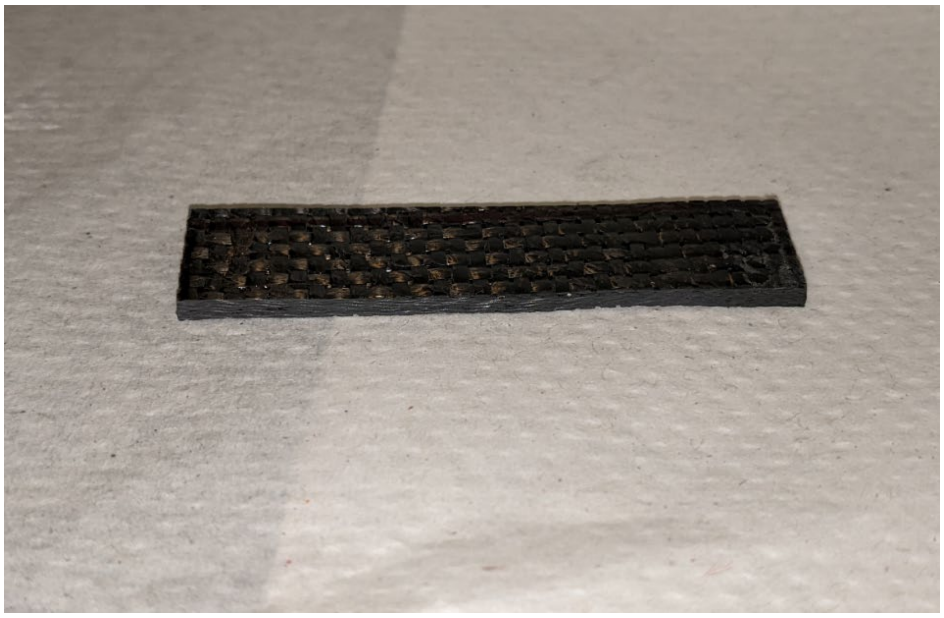

Figure A1: CFRP Exposure Coupon

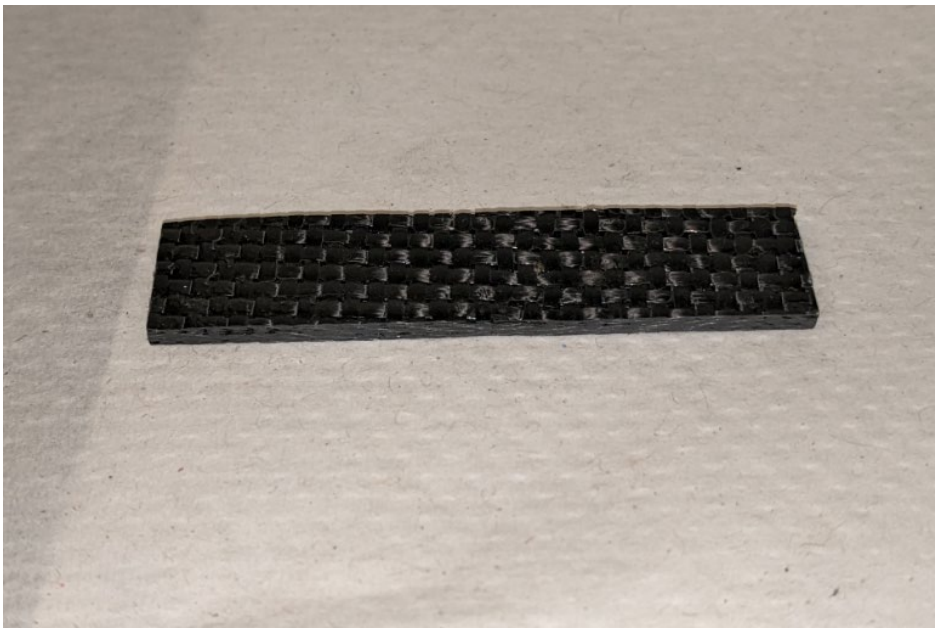

Figure A2: CFRP Unexposed Coupon

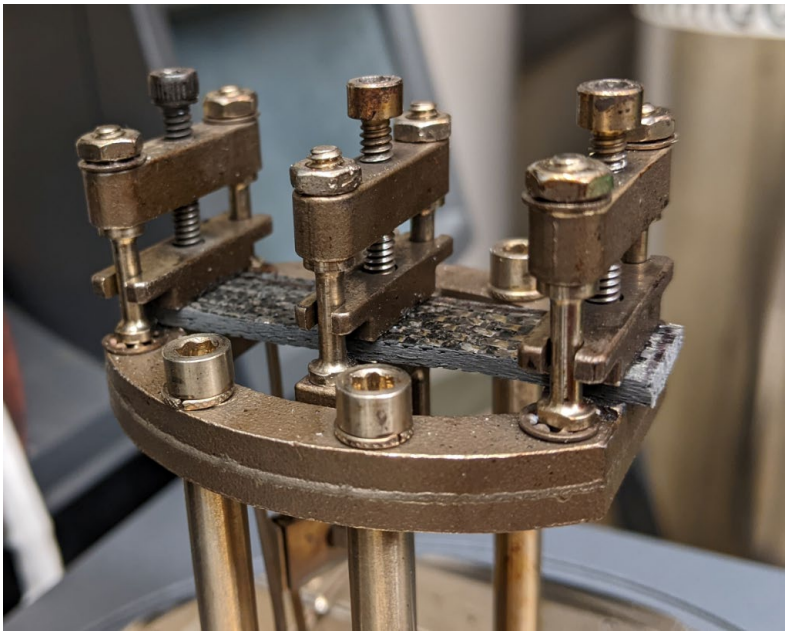

Figure A3: DMA Dual Cantilever with CFRP Exposed Coupon

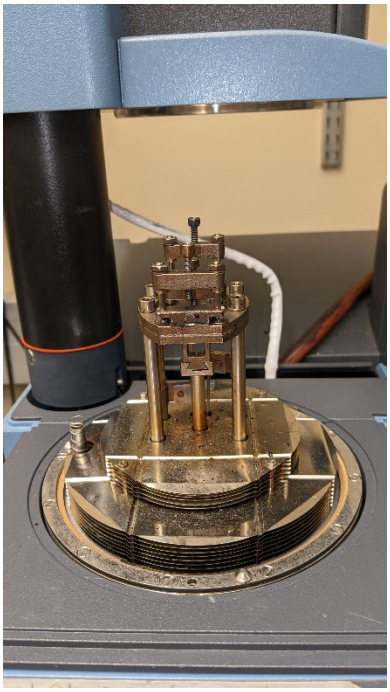

Figure A4: DMA Set up for test runs

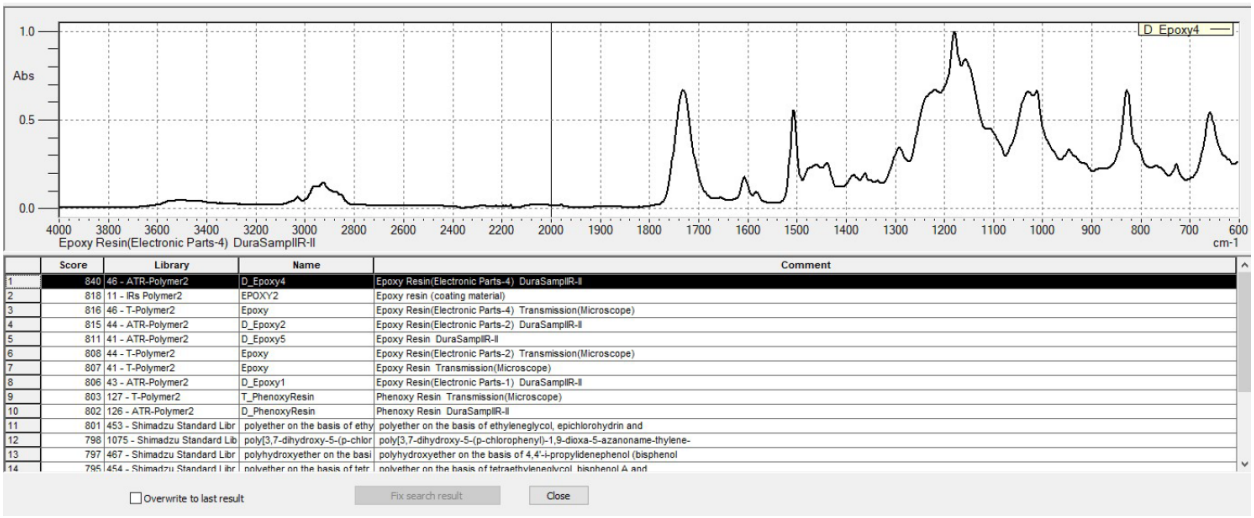

	Score	Library	Name	Comment
1	840	46 - ATR-Polymer2	D_Epoxy4	Epoxy Resin(Electronic Parts-4) DuraSamplIR-II
2	818	11 - IRs Polymer2	EPOXY2	Epoxy resin (coating material)
3	816	46 - T-Polymer2	Epoxy	Epoxy Resin(Electronic Parts-4) Transmission(Microscope)
4	815	44 - ATR-Polymer2	D_Epoxy2	Epoxy Resin(Electronic Parts-2) DuraSamplIR-II
5	811	41 - ATR-Polymer2	D_Epoxy5	Epoxy Resin DuraSamplIR-II
6	808	44 - T-Polymer2	Epoxy	Epoxy Resin(Electronic Parts-2) Transmission(Microscope)
7	807	41 - T-Polymer2	Epoxy	Epoxy Resin Transmission(Microscope)
8	806	43 - ATR-Polymer2	D_Epoxy1	Epoxy Resin(Electronic Parts-1) DuraSamplIR-II
9	803	127 - T-Polymer2	T_PhenoxyResin	Phenoxy Resin Transmission(Microscope)
10	802	126 - ATR-Polymer2	D_PhenoxyResin	Phenoxy Resin DuraSamplIR-II
11	801	453 - Shimadzu Standard Libr	polyether on the basis of ethy	polyether on the basis of ethyleneglycol, epichlorohydrin and
12	798	1075 - Shimadzu Standard Lib	poly[3,7-dihydroxy-5-(p-chlor	poly[3,7-dihydroxy-5-(p-chlorophenyl)-1,9-dioxa-5-azanoname-thylene-
13	797	467 - Shimadzu Standard Libr	polyhydroxyether on the basi	polyhydroxyether on the basis of 4,4'-i-propylidenephenol (bisphenol
14	795	454 - Shimadzu Standard Libr	polyether on the basis of tetr	polyether on the basis of tetraethyleneglycol, bisphenol A and

Overwrite to last result Fix search result Close

Figure A6: HiMassSEE CR-39 ground control coupon view after 924 day ground controls (same duration as flight samples), no foil

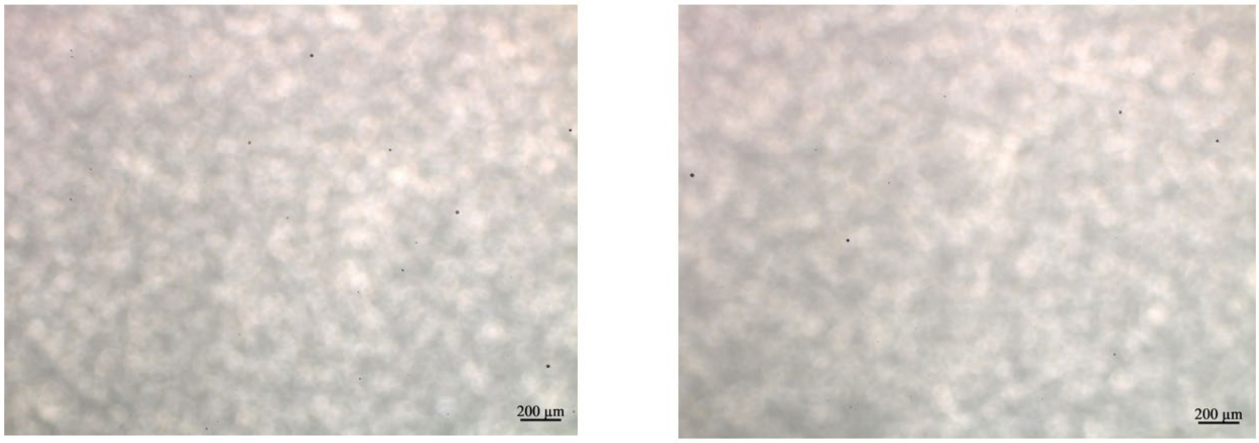

Figure A5: FTIR Material Classification as being a Epoxy

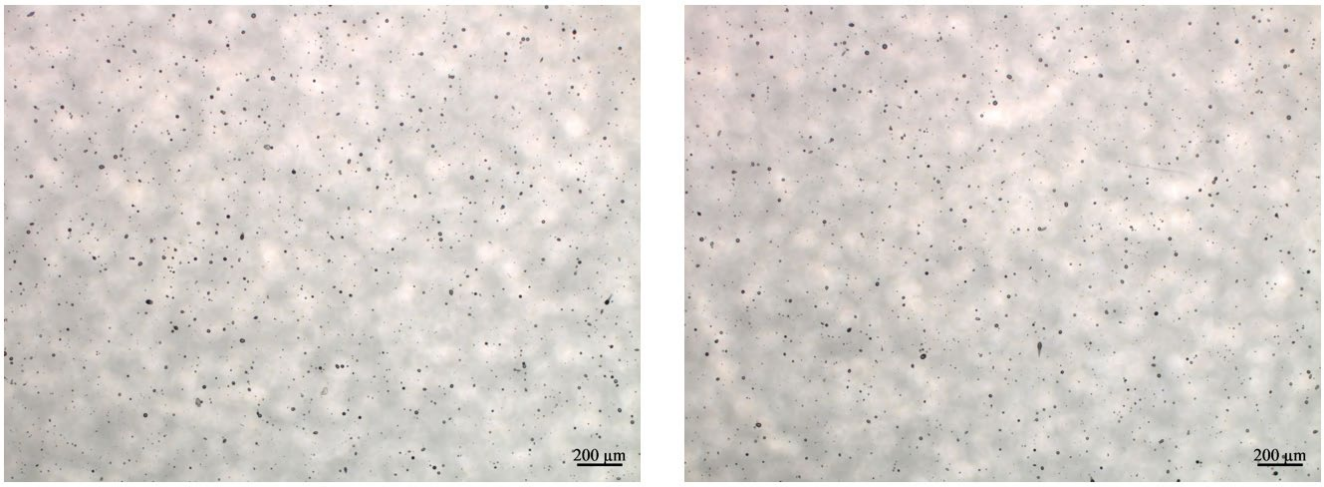

Figure A7: HiMassSEE CR-39 flight control (no metal foil) after 924 days in orbit inside the pressurized volume of ISS

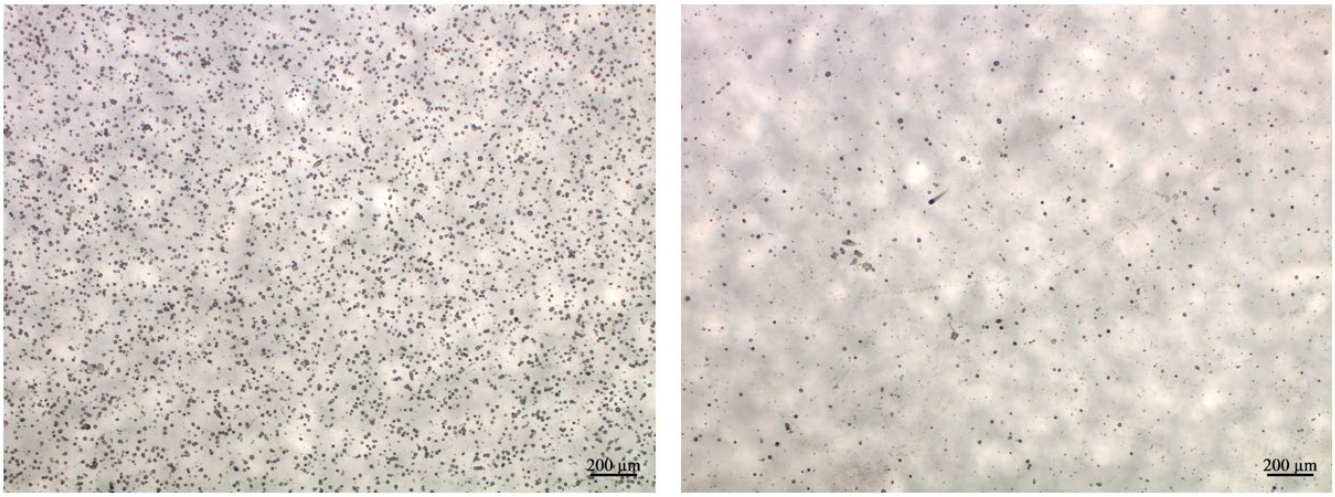

Figure A8: HiMassSEE CR-39 Coupon with Lead Foil (Left) and no metal foil (Right) after 924 days in orbit inside the pressurized volume of ISS

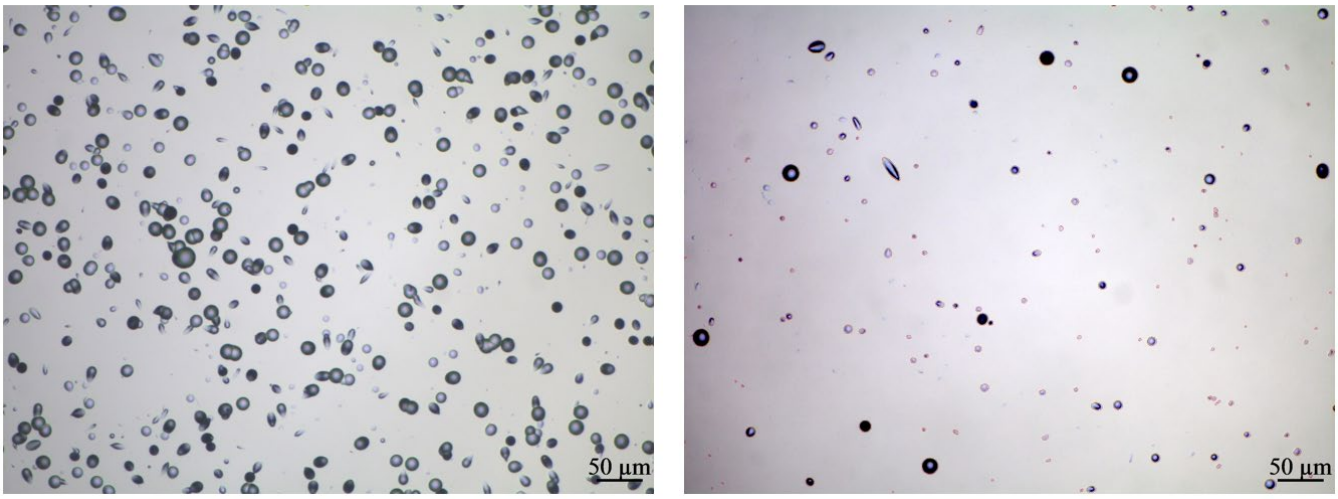

Figure A9: HiMassSEE CR-39 Coupon with Lead Foil (Left) and no metal foil (Right) after 924 days in orbit inside the pressurized volume of ISS

VITA

Ian David Juby

Candidate for the Degree of

Master of Science

Thesis: EFFECT OF SPACE RADIATION ON COMPOSITE MATERIAL THAT WAS INTERNAL AND EXTERNAL OF THE PRESSURIZED VOLUME ON THE INTERNATIONAL SPACE STATION (ISS)

Major Field: Material Science and Engineering

Education:

Master of Science (July 2022) in Materials Science and Engineering, Oklahoma State University, Tulsa, OK

Bachelor of Science (Dec 2013) in Mechanical Engineering, Oklahoma State University, Stillwater, OK

Academic Employment:

Graduate Research Assistant, Department of Materials Science and Engineering, Oklahoma State University, January 2014 – August 2015. Research activities included work on multiple grants dealing with composite structures or composite overwrapped pressure vessels. Research and design in thermo materials for insulating medical containment solutions.

Professional Memberships:

AIAA (American Institute of Aeronautics and Astronautics) - Voting Member
CSA Group – Voting Member